275
8-6-80

MASTER

I-Dn.1609

SAND 79-2422
Unlimited Distribution

THE EFFECT OF SOILING ON SOLAR MIRRORS AND TECHNIQUES USED TO MAINTAIN HIGH REFLECTIVITY

(To be published in a book entitled Solar Energy Materials
ed: L. E. Murr (Academic Press, 1980)).

E. P. Roth, R. B. Pettit

Prepared by Sandia Laboratories, Albuquerque, New Mexico 87185 and Livermore, California 94550 for the United States Department of Energy under Contract AT(29-1)-789

June, 1980

Sandia National Laboratories

SF 2900-Q(3-80)

Issued by Sandia National Laboratories, operated for the United States Department of Energy by Sandia Corporation.

Printed in the United States of America

Available from
National Technical Information Service
U. S. Department of Commerce
5285 Port Royal Road
Springfield, VA 22161

Price: Printed Copy $5.25; Microfiche $3.00

THE EFFECT OF SOILING ON SOLAR MIRRORS AND TECHNIQUES USED TO MAINTAIN HIGH REFLECTIVITY

TABLE OF CONTENTS

Figure Captions

Fig. 1. Specular reflectance of second-surface silvered glass mirrors exposed to natural weathering for 480 days. Reflectance measured at 500 nm and 15 mrad angular aperture.

Fig. 2. Expected long-term reflectance of an exposed mirror with and without periodic cleaning.

Fig. 3. Specular reflectance of mirrors undergoing (a) 2-day, (b) 6-day and (c) 12-day cleaning cycles. The dashed lines show the reflectance increase due to laboratory cleaning; the solid lines show the reflectance loss due to natural soiling.

Fig. 4. Specular reflectance of 5 mirrors as a function of mounting angle (0° = face up; 180° = inverted). The mirrors were exposed for a total of 127 hours (≈5 days) during daylight hours of good weather.

Fig. 5. Hemispherical reflectance for a clean, second-surface, silvered float glass mirror.

Fig. 6. Specular reflectance as a function of wavelength for an initially clean mirror (upper curve) and after increasing levels of dust accumulation (lower curves). Values listed are the specular reflectance loss measured at 500 nm for a 15 mrad angular aperture due to dust accumulation.

Fig. 7. Specular reflectance loss due to soiling normalized by the specular reflectance of the clean mirror as a function of wavelength. (R_D = Dirty mirror, R_C = Clean mirror). The functional dependence of the normalized reflectance loss is directly proportional to the scattering strength of the accumulated dust. The data are obtained from the curves in Fig. 6 for the various levels of dust accumulation. The values listed refer to the specular reflectance loss at 500 nm.

Fig. 8. Diffuse reflectance as a function of wavelength for the soiled mirrors shown in Fig. 6. The values listed refer to the specular reflectance loss at 500 nm.

Fig. 9. Diffuse reflectance normalized by the diffuse reflectance at 500 nm as a function of wavelength for all levels of soil accumulation shown in Fig. 8. The High and Low curves represent the limits of the normalized curve due to the uncertainty in each measurement. The High and Low solar average values refer to the limits of the solar averaged specular reflectance loss as discussed in the text.

Fig. 10 Specular reflectance as a function of angular aperture for a clean mirror (upper curve) and for increasing levels of dust accumulation. The difference values listed are the difference in specular reflectance between 3 mrad and 15 mrad. The losses listed at the right are the specular reflectance losses measured at 15 mrad. All data were measured at 500 nm.

Fig. 11 Extinction coefficient calculated from Mie scattering theory for a spherical particle with index of refraction m = 1.5 as a function of the size parameter $X = 2\pi r_p/\lambda$ where r_p = particle radius and λ = wavelength of incident light.

Fig. 12. Amplitude of scattered light as a function of angle for a spherical particle with index of refraction m = 1.55 and size parameter $x = 2\pi r_p/\lambda = 3.0$. The angle of the incident light is 0°.

Fig. 13 (a) Schematic of light scattering by dust particles on a second-surface mirror where I_o = incident light, I_s = scattered light and I_r = reflected light. (b) Convolution of wavelength dependent extinction coefficient and the solar spectral distribution as a function of particle diameter. (c) Particle size distribution function for a naturally soiled mirror.

Fig. 14 Energy loss as a function of particle size assuming a particle size distribution function $n(r) \propto r^{-3}$ (solid curve). Energy loss assuming a dropoff in the particulate concentration for $r_p \lesssim 0.2$ µm (dashed curve). The incident radiation is assumed to have the standard solar distribution at sea level.

Fig. 15 Particle size distribution functions for naturally soiled mirrors. Open circles: mirror exposed to natural cleaning (wind and rain) for several months. Open squares: mirror exposed only to "good" weather conditions for a period of 2 days.

Fig. 16 Accelerated deposition wind tunnel with laser optics for monitoring particle flux and measuring real-time reflectance loss of exposed mirror.

Fig. 17 Normalized real-time reflectance loss for mirrors exposed to a particle flux of $\approx 1.2 \times 10^5$ particles/cm^2-sec at wind velocities of 20 MPH (Mirror A) and 25 MPH (Mirror B).

THE EFFECT OF SOILING ON SOLAR MIRRORS AND TECHNIQUES USED TO MAINTAIN HIGH REFLECTIVITY*

E. P. Roth and R. B. Pettit
Sandia Laboratories**
Albuquerque, New Mexico 87185

I. Introduction

Solar mirrors are used to concentrate low-level solar radiation to power levels which are practical and efficient for consumption. Any interference with the collection of that energy not only decreases the power level but also increases the cost of the energy available from a solar power system. Solar mirrors are designed to initially achieve the maximum possible reflectance. However, outdoor exposure subjects the mirror materials to environmental conditions which can quickly degrade their efficiency. One of the most immediate and drastic effects of outdoor exposure is the reflectance loss due to the accumulation of foreign particles on the mirror surface. Specular reflectance losses as great as 25% have been observed for mirrors exposed for only a few weeks. The effect of the deposited particles is to reduce the reflected energy by both absorbing and scattering light.(1,2) The degree to which the particles reduce the collection of reflected energy depends on their composition, number and size distribution.(1,2) An additional factor is the optics of the collection system. The angular acceptance aperture of the system, defined as the angle subtended by the receiver at the concentrator surface, determines the relative importance of the scattering due to dust accumulation. For flat plate thermal and photovoltaic collectors which have essentially a 180° angular acceptance aperture, scattering of the incident light is not critical but absorption can be an important factor in the loss of energy. For concentrating collection systems,

*This work is supported by the Division of Solar Technology, U.S. Department of Energy (DOE), under contract DE-AC04-76-DP00789.
**A U.S. DOE facility.

such as line focus collectors and central receivers, angular acceptance apertures of a few degrees make scattering at the concentrator surface much more important and can result in severe energy losses. Thus, from an economic point of view, periodic cleaning or reduction of soil accumulation is a practical necessity.

II. Effect of Natural Soiling on Mirror Reflectance

Potential methods for controlling the reflectance loss due to soiling must be based on both measurements of actual particulate accumulation in an outdoor environment and an understanding of the basic physical mechanisms of adhesion and light scattering. In order to establish a data base for the reflectance loss of exposed mirrors, a field test study was initiated simulating some of the operational configurations of solar mirrors.

A. Long Term Soil Accumulation Study

Solar mirror materials have been exposed to natural weathering in Albuquerque, NM for periods exceeding one year.[3] The mirror materials used were second-surface silvered glass obtained from a heliostat panel at the 5MW Central Receiver Test Facility (CRTF) at Kirtland AFB, Albuquerque, NM.[4] These samples are typical of the type of materials used in many solar thermal power systems. The specular reflectance of the mirrors was measured with a bidirectional reflectometer over a wavelength range 400-900 nm and over a 3-15 mrad range of angular acceptance apertures.[5] Figure 1 shows the specular reflectance data for a mirror exposed for 480 days to natural weathering.[6] The data shown are for a wavelength of 500 nm and a 15 mrad angular aperture. The data show an initial rapid drop in reflectance of approximately 0.006 reflectance units per day (100% reflectance = 1.00 reflectance units) followed by large fluctuations in reflectance which are induced by variations in weather conditions. The weather condition at a particular mirror location is one of the critical factors affecting the rate of dust accumulation and the eventual long term reflectance loss of an exposed mirror. Daily reflectance losses as great as 0.144 reflectance units have been measured under certain conditions (light rain followed by a wind and dust storm) while increases as large as 0.121 reflectance units have been measured at other times (snow-rain weather conditions).(6)

Because of the variation in local weather, it is very difficult to predict long term reflectance losses for a given location and more difficult to apply those results to other locations. In general, uncleaned mirrors in the Albuquerque area show a long term decrease in specular reflectance of approximately 0.10-0.15 reflectance units with large fluctuations about the average.(3) Larger reflectance losses can occur in other geographic locations, especially in urban environments where optically absorbing particles from pollutants can lead to additional energy losses.(7) Additional outdoor exposure studies at other geographic locations are required to obtan a more general understanding of mirror soiling.

B. Cleaning Cycle Experiment

When the reflectance of a solar mirror drops sufficiently, cleaning the mirror surface becomes economical. Increasing the cleaning frequency should raise the average long-term reflectance of the mirror, as depicted in Figure 2, although some long-term degradation may result from the cleaning procedures. Figure 3 shows the results of actual cleaning cycle tests in which three sets of mirrors were exposed and cleaned on 2-, 6- and 12-day cycles.(3) The mirrors were measured every two days to show any fluctuations due to weather conditions. The results show that laboratory cleaning (three minutes in an ultrasonic bath of distilled water and wiped dry with a soft tissue) essentially restores the reflectance of each mirror to its initial value. Subsequent exposure results in a rapid nonlinear drop in reflectance for each set of mirrors. The average daily reflectance loss for, respectively, the 2-, 6- and 12-day cycle mirrors was

0.0085, 0.0061 and 0.0051 reflectance units. Thus, the rate of dust accumulation decreases as the amount of accumulated dust increases. The long term average reflectance loss for the 2-, 6- and 12-day cycled mirrors is, respectively, 0.0085, 0.018 and 0.031 reflectance units, indicating that increased frequency of cleaning does raise the average reflectance of the mirrors.

The level of dust accumulation is also seen to affect the response of the mirrors to weather conditions.[3] For example, mirrors which had an appreciable accumulation of dust were cleaned by a light rain while newly cleaned mirrors experienced a loss in reflectance under the same conditions. These results show that weather and mirror conditions can significantly affect the reflectance of exposed mirrors and that these conditions must be fully considered in any method to predict long-term reflectance loss.

C. Orientation Angle Experiment

Several operational parameters can affect the rate of soiling of exposed mirrors. For example, the orientation angle of a mirror during periods of inoperation can affect the rate of particulate settling on the surface and can maximize the effect of natural cleaning forces such as wind and rain. To investigate the effect of stowage angle on mirror degradation, a set of five mirrors was exposed on a test rack at different angles with respect to the horizontal: 0°, 30°, 45°, 60° and 180° (inverted).[3] These samples were exposed only during daylight hours of good weather, thus representing soiling strictly due to dry deposition. The results of this experiment are shown in Figure 4. Generally, the drop in specular reflectance decreased as the orientation angle increased; however, only the inverted (180°) mirror showed a significant reduction in soiling. In other experiments, a 90° stowage angle has also resulted in a significant decrease in the rate of soiling.[8] These experiments show that any method formulated to maintain high reflectivity of solar mirrors must involve the optimization of both the cleaning cycle and the stowage position.

III. Effect of Accumulated Dust on Specular Reflectance

The detailed interaction of accumulated dust with the incident solar radiation is important in understanding and predicting the loss in collected energy. Measurements were performed on a set of solar mirrors exposed to natural weathering for a period of five weeks to determine the wavelength dependent scattering by the particulates and the effect of the dust on the beam shape of the scattered light.(9)

A. Hemispherical Reflectance

Initially, the hemispherical reflectance of a clean mirror was measured over the wavelength interval 320-2500 nm using an integrating sphere reflectometer.(10) This device allows collection of both the specular and diffuse component of the reflected beam over a solid angle of 2π steradians. Typical data are shown in Figure 5. The large dip in reflectance at 1000 nm is due to absorption in the glass by Fe^{+2} impurities.(11) The cutoff below 400 nm results from losses in the glass and in the silver reflector layer.(12) Subsequent measurements of hemispherical reflectance after soiling showed no appreciable decrease in reflectance for specular reflectance losses up to ≈ 0.05 reflectance units, indicating that the energy lost from the specular component went into the diffuse scattering background with no measurable loss due to absorption. These results are consistent with the type of losses expected from dielectric (nonconducting) particles which are usually found in a desert environment. However, outdoor exposure to urban environments could lead to contamination by absorbing pollutants which could cause a decrease in the net hemispherical reflectance.(7)

B. Wavelength Dependence

The specular reflectance of mirrors with increasing levels of dirt accumulation is shown in Figure 6 over the wavelength range of 400-900 nm measured at a 15 mrad aperture.(9) The dominant effect of the accumulated dust is the decrease in specular reflectance over the entire wavelength range with increasing level of dust accumulation. At 500 nm the specular reflectance loss varied from 0.065 to 0.24 reflectance units. The wavelength dependence of the specular reflectance loss is shown in more detail in Figure 7. In this figure, the specular reflectance loss R_D-R_C, is normalized by the reflectance value of the clean mirror, R_C at each wavelength. The wavelength dependence of the reflectance loss is directly proportional to the scattering cross section of the dust particles. The data show that the net scattering by the accumulated particles increases with decreasing wavelength and with increasing level of soiling, with the scattering amplitude still increasing at 400 nm. Since the soil particles accumulated in this experiment do not result in any appreciable absorption, the light lost from the specular beam forms the diffusive reflection background. The wavelength dependence of the diffusive background is shown in Figure 8 for the levels of soil accumulation shown originally in Figure 6. The diffusive scattering was measured with the integrating sphere reflectometer over the wavelength range 320-2500 nm. Because of differences in the beam sizes, collection apertures and measurement regions, the loss in specular reflectance and the increase in diffuse reflectance are not in exact agreement. However, by normalizing the diffuse reflectance by the value at 500 nm, the wavelength dependent scattering can be approximately determined, independent of the degree of soiling. The resulting normalized curve is shown in Figure 9. The HIGH and LOW curves represent the maximum and minimum normalized loss values respecively from all regions measured. This figure shows that within the accuracy of the data the wavelength dependence of the scattering is independent of the concentration of accumulated particles. This result is useful since it allows a solar-averaged reflectance loss for this silvered glass mirror to be calculated from a measurement at a single wavelength. For the type of mirrors used in this experiment, the solar averaged reflectance loss is equal to 0.78 ± 0.04 times the specular reflectance loss measured at 500 nm.

C. Effect of Dust Particles on Beam Shape

Accumulated dust particles can have a significant effect on the performance of a solar collector with a small angular acceptance aperture by affecting the shape of the reflected beam. The effect of accumulated particles on beam shape was measured using the laboratory bidirectional reflectometer over an angular aperture range of 3-15 mrad.[9] The data are shown in Figure 10 at the standard wavelength of 500 nm for increasing levels of dust accumulation. The values listed in the figure are the differences in specular reflectance between the 3 and 15 mrad measurement points. The data show that the main effect of accumulated dust is to decrease the overall intensity of the reflected beam and not to significantly change the profile. Wide-angle scattering by the accumulated particles (scattering at angles much greater than the acceptance aperture of the collection optics) can account for this effect and result in comparable losses for both central receiver and distributed power systems which both have apertures $\lesssim 2°$.

IV. Scattering Theory

The detailed scattering of light by particles is a complex function of the optical properties of the particles, the size and number distribution of the particles, and the wavelength of the incident light.[1,2] For solar power systems, the incident light comes from direct radiation by the sun. The wavelength distribution of the solar radiation may be modeled as a black body spectrum corresponding to a temperature of ≈5800 K, modified by absorption in both the solar and terrestrial atmospheres.[1,3] The peak in the atmospheric spectrum occurs at approximately 500 nm, with a lower cutoff at 300 nm and an upper cut off at 3500 nm.

A. Extinction Coefficient and Angular Scattering Function

The scattering of light by a single particle is a function of the particles' complex index of refraction, the particle shape and the size of the particle compared to the wavelength of the incident light.[1,2] The efficiency of a particle in removing energy from incident light is derived from Mie scattering theory and is given by its extinction coefficient:

$$K_{EXT} = K_{SCAT} + K_{ABS} \tag{1}$$
$$= \sigma_{SCAT}/\sigma_A + \sigma_{ABS}/\sigma_A \quad ,$$

where K_{SCAT} is the ratio of the effective scattering cross section (σ_{SCAT}) of the particle to its actual geometric cross section (σ_A) and K_{ABS} is the ratio of the effective absorption cross section (σ_{ABS}) to the geometric cross section. The extinction coefficent for a spherical dielectric particle (no absorption) is shown in Figure 11 as a function of the particle circumference/wavelength ratio.[1,2] This curve is valid for most particles of interest for which $1 \lesssim m \lesssim 2$ where m is the complex index of refraction. The figure shows that the extinction coefficient drops off rapidly for particles small compared to the wavelength of the incident light, peaks at a value where the particle size is comparable to the wavelength and then undergoes oscillations of decreasing amplitude about a value of ≈ 2 with increasing particle circumference/wavelength ratio. For increasing magnitude of the index of refraction, the peak in the extinction coefficient shifts to longer wavelengths.[1,2]

The angular distribution of the scattering energy is a complicated function of the relative particle circumference/wavelength ratio, particle index of refraction and polarization of the incident light.[2] Figure 12 shows the scattering amplitude as a function of angle for a particle with 1.55 index of refraction and with circumference/wavelength ratio $2\pi r_p/\lambda = 3.0$ (r_p = particle radius). As the size of the particle becomes equal to or larger than the wavelength of the incident light the scattering amplitude becomes peaked in the forward direction with weaker lobes occurring at larger angles. However, for most naturally occurring particles, the majority of the scattered energy still occurs at angles greater than the few degree angular acceptance apertures of most concentrated power systems. These calculations agree with the large-angle scattering which previously accounted for the negligible effect of accumulated dust on the shape of the specularly reflected beam profile.

B. Loss in the Specular Reflection Component

The loss in the specular component of reflected solar energy due to scattering by dust particles can be calculated by convoluting the particle extinction coefficients, particle size distribution and solar spectral distribution over all particles sizes and solar wavelengths.[1] The expression for this loss is given as

$$\Delta I_m/I_o = 2\int_0^\infty dr \int_0^\infty d\lambda \left\{\pi r^2 K_{EXT}\left(\frac{2\pi r}{\lambda}, m\right) n(r,m)\, f(\lambda)\right\}$$

$$= 2\int_0^\infty dr \left\{\pi r^2 \dot{n}(r,m) \int_0^\infty K_{EXT}\left(\frac{2\pi r}{\lambda}, m\right) f(\lambda)\, d\lambda\right\} , \qquad (2)$$

where r = particle radius, n(r,m) = number of particles/unit area-unit radius, m = complex index of refraction, I_o = solar spectral intensity and $f(\lambda)$ = wavelength function of the solar spectrum. In this expression, the incident solar radiation is assumed to have interacted with the surface layer of dust particles twice as shown schematically in Figure 13a. The result of convoluting the wavelength dependent extinction coefficient for a spherical particle with m = 1.5 and the solar distribution function is shown in Figure 13b. The net loss in intensity of the specular beam is then obtained by further convoluting the function shown in Figure 13b with the particle area and the particle size distributions function shown in Figure 13c. The particle size distribution function shown in this figure is representative of the distribution function actually measured on exposed mirrors. This function will be discussed in more detail in Section V, B. The resultant energy lost from the specular beam per unit particle diameter; i.e., the integrand in the second line of Eq. (2), is shown in Figure 14, assuming a particle distribution function of the form $n(r,m) \propto r^{-3}$ for ease of calculation. The peak in energy loss occurs near 500 nm, corresponding to the peak in the solar spectrum. This analysis emphasizes the importance of the small particle ($0.05\ \mu m \lesssim r_p \lesssim 1\ \mu m$) in the scattering loss. A decrease in the number density of small particles ($r_p \lesssim 0.2\ \mu m$), which has been measured by some investigators, would cause a sharper cutoff in the energy loss function for the small particle diameters, as shown by the dashed curve in Figure 14. However, the major loss of energy still results from particles in the submicron range.

V. Deposition and Adhesion

The deposition of particles on a mirror surface is controlled by the complex fluid mechanical interaction of the dust-laden airstream with the entire mirror structure.[14] Processes such as convective diffusion, impaction and sedimentation play important roles in the deposition process depending on particle size and wind velocity. In general, particles whose Stokes velocity is less than the ambient wind velocity will be carried to the mirror surface and can be subsequently deposited. Particles with diameters $\lesssim$ 100 microns will be suspended by wind velocities of only a few miles per hour resulting in a broad size spectrum of deposited particles.

A. Forces of Adhesion

A wide range of forces are responsible for the adhesion of the particles to the surface, as listed in Table 1. The magnitude of these forces depends strongly on the nature of both the particles and the mirror surface, varying from a fraction of the gravitational force on the particle to several orders of magnitude greater than the gravitational force.[15] The details of these different mechanisms are not sufficiently well understood to permit accurate estimations of the type and magnitude of forces responsible for particle adhesion. However, the initial forces of adhesion are probably dominated by electrostatic forces and surface energetics, while after sufficiently long periods of time stronger chemical and physical bonds can develop. The few experiments that have been performed show that the forces of adhesion in general increase with decreasing particle size and with increasing time of surface contact.[15] The development of the stronger chemical bonds will depend strongly on the amount of moisture present at the particle mirror interface and are thus affected by such parameters as relative humidity and rainfall.

B. <u>Particle Distributions</u>

As discussed in Section IV, B, the small particles ($r_p \lesssim 1$ μm) are the most important source of scattering for the solar spectrum and, as stated in the previous section, experience the greatest surface adhesion. Measurements of the actual particle size distribution on weathered mirrors can yield information on the relative significance of the various particle sizes and how different environmental conditions can affect their rates of accumulation.

Particle size distributions have been measured using a Quantimet particle sizer.[16] This instrument measures the number of particles in selected size intervals from direct optical images of the mirror surface and from high magnification micrographs taken on a scanning electron microscope. Overlapping particle size measurements are made at different magnifications at several random locations on the surface to obtain a representative characterization of the entire mirror surface. An average of 60-70 different locations are measured using five different magnifications covering particles with diameters $\gtrsim 0.3$ μm. A typical particle distribution for a mirror subjected to several months of outdoor exposure is shown by the open circles in Figure 15. For convenience in comparing to atmospheric aerosol distributions reported in the literature, the size distribution is presented as a logarithmic function,

$$dN/Ad(\log r) \quad (cm^{-2}) \quad , \tag{3}$$

where N is the number of particles with radii < r, r is the particle radius and A is the unit area of mirror surface.[17-19] In general, the size distribution is described as

$$dN/Ad(\log r) \propto r^{-k} \quad , \tag{4}$$

where $k \approx 2$ for this sample. The particle distribution measured in atmospheric aerosols for particle radii $\gtrsim 1$ μm is usually described by a power law distribution. The actual logarithmic slope can vary significantly depending on location, weather and time of year.[17-19] Below 1 μm the atmospheric particle distribution function usually levels off or actually decreases. The entire distribution is often referred to as a lognormal distribution which is modeled with a logarithmic Gaussian function plus a power law background distribution.[18] The distribution of particles accumulated on the exposed mirror shows some deviation from the power law distribution function below 1 μm but the decrease is smaller than observed in aerosols, indicating some preferential adhesion of the small particles out of the atmospheric distribution. This result is consistent with experiments which have shown increased adhesion for small particles.[15]

If indeed the small particles adhere more strongly to the mirror surface, then the small particles should likewise be more difficult to remove. The result of preferential adhesion of the small particles can be seen by comparing the particle distribution of the weathered mirror to the distribution of a mirror which has undergone only dry deposition. The open squares in Figure 15 show the particle distribution for a mirror which has undergone only two days of exposure during dry weather. The measured slope is ≈ -1.1 compared to ≈ -2.1 for the weathered mirror. The greater magnitude of the slope of the weathered mirror occurs because of "natural" cleaning conditions, such as wind and rain, which preferentially remove the larger particles while the relative number of smaller particles continue to increase. This result has been confirmed by measurements on other mirrors which have undergone varying lengths of outdoor exposure to both "dry" and "wet" environments.

VI. Accelerated Deposition Study

Variations in weather conditions cause such large fluctuations in the reflectance of exposed mirrors that long-term predictions of reflectance loss are difficult to make. Measurement of reflectance loss and particle accumulation under controlled conditions can yield a better understanding of the effect of such parameters as wind velocity, particle flux and humidity on the rate of reflectance loss. In addition, controlled particle deposition allows an accurate comparison of soiling rates for various mirror materials and cleaning techniques.

A. Wind Tunnel

Representative mirror materials have been exposed to accelerated dust deposition in a low-velocity wind tunnel equipped with a dust injector/disperser unit and laser optical systems capable of monitoring the flux rate of the incident particles and the real-time reflectance loss of the exposed mirrors. The mirrors are exposed to controlled amounts of a well-defined Arizona Desert Dust[20] over velocity ranges of ≈10-30 MPH. The samples are mounted normal to the incident airstream to achieve the maximum rate of dust accumulation. The dust injector/disperser unit is capable of injecting particles at densities $\approx 10^4$ times greater than the particle densities present in normal atmospheric aerosols. The injector has also been designed to maintain a constant injected particle size distribution over the period of deposition. Specular reflectance losses observed after several months of outdoor exposure have been simulated in approximatly 30 minutes in the wind tunnel. Although this accelerated deposition system is not intended to exactly duplicate outdoor exposure, it does allow a comparative measurement of dust accumulation on various materials under a wide range of exposure conditions.

B. Laser Optics

The dust-laden airstream is monitored using a laser velocimeter apparatus and a multichannel analyzer to record the flux of incident particles during the deposition period, as shown in Figure 16. The green beam (λ = 0.5145 nm) from an argon laser is split into two components and recombined in front of the exposed mirror to form a region of interference fringes. As particles pass through the sampling volume, they scatter light with an intensity pattern characterized by the spacing of the interference fringes and the particle velocity, thus allowing the particle transit to be distinguished from background noise in the phototube[(21)]. Typical flux levels range from 5×10^4 - 5×10^5 particles/cm^2-sec.

During the deposition, the reflectance of the mirror is monitored using a He-Ne reflectometer. A He-Ne laser beam is expanded to approximately 1 cm diameter and is split into a sample beam and a reference beam. The two beams (45° to the mirror surface) follow identical optical paths through the wind tunnel so that any loss in intensity due to the dust-laden airstream is equal for both beams. The ratio of the intensity of the sample beam to the reference beam yields the normalized specular reflectance of the mirror independent of fluctuations in the laser beam intensity. The reflectance losses measured with this system have been compared with specular reflectance losses measured with a laboratory bi-directional reflectometer at 633 nm and agreement has been found to be within 0.013 reflectance units over a loss range of 0.05-0.9 reflectance units. A typical reflectance loss curve as a function of deposition time is shown in Figure 17 for a second-surface silvered glass mirror (mirror A). This particular deposition was performed at a wind velocity of 20 MPH and a flux rate of $\approx 1.2 \times 10^5$ particles/cm^2-sec. Note that the reflectance loss is approximately a linear function of deposition time. An identical mirror (mirror B) was exposed to the same particle flux but at a velocity of 25 MPH, also shown in Figure 17. At this higher velocity, the rate of reflectance loss decreased by a factor of ≈ 1.8. The variation of this single parameter shows that the reflectance loss rate is a rather strong function of wind velocity under conditions of dry deposition. This effect results from the increased kinetic energy of the particles at higher wind velocities which causes the particles to rebound from the surface rather than be held by the acting forces of adhesion.(15) A change in velocity should have the greatest effect on the small particles which undergo the greatest deacceleration along the stagnation line of the mirror. Increasing the kinetic energy of these particles raises their energy above the effective "capture threshold" energy of the mirror and results in a drop in the effective "sticking coefficient" of the small particles. The energy of a significant number of the larger particles at low velocities already would exceed the "capture threshold" of the mirror so that they would be less affected by a change in velocity. Initial measurements of the particle distribution on these two mirrors indeed show a significant increase in the relative numbers of small particles ($r_p \lesssim 5$ μm) for mirror A (V = 20 MPH) compared to mirror B (V = 25 MPH). The 1 μm particle density ratio of mirror A to mirror B was ≈ 3.1 while the ratio was ≈ 1.3 at a radius of 10 μm. These results again point to the significant role of the small particles in determining the reflectance loss of exposed mirrors. Experiments are currently being conducted to extend the scope of these controlled depositions to include other mirror materials, coatings and exposure conditions.

VII. Cleaning Strategies

An understanding of the mechanisms of dust deposition and adhesion can lead to the development of techniques to maintain high reflectivity under outdoor exposure conditions. Current cleaning strategies can be generalized into the following categories:

1) Keep dirt from settling and adhering to the surfaces.
2) Wash off dirt with water or low surface energy detergent-type solutions before strong chemical or mechanical bonding can develop.
3) Wash off dirt with chemically or mechanically active cleaning techniques capable of breaking the chemical and mechanical bonds that have developed.
4) Modify the surface so that strong bonding cannot develop.

The above strategies can be divided generally into either active or passive cleaning methods. Active cleaning methods (strategies 2 and 3) are labor intensive techniques which can have serious economic restrictions on the operation of a solar power system, while passive techniques (strategies 1 and 4) are primarily capital intensive and can possibly result in lower, long-range cleaning costs. Currently, strategies 1 and 4 are being investigated as possible approaches to the soiling problems, encompasing such techniques as ultrasonic vibration, electrostatic biasing and antistatic, antisoiling surface coatings.[22,23]

Investigation of strategies 2 and 3 has indicated that glass mirrors can be cleaned to within 2% and acrylic mirrors to within 8% of their initial reflectance using a high-pressure (1000 psi) tap water spray. In locations containing hard water, a final rinse with deionized water or tap water containing a sheeting agent may be required. Mechanically or chemically active cleaning is required to restore 100% of the initial mirror reflectance. However it is not clear if there may be some long-term buildup of nonremovable soil of degradation of the mirror surface due to cleaning.[24]

Preliminary tests using conducting oxide coatings, [(SnO_2) coupled with an electrostatic field] have resulted in the reduction of dust accumulation during wind tunnel exposures.[14] More extensive experiments are planned using this technique to characterize the independent effects of the coatings and the applied fields on the rate of dust accumulation and the particle size distributions. Eventually this technique will be applied to field test experiments.

VIII. Conclusions

The accumulation of dust and the resulting loss in specular reflectance of exposed mirrors is a complex function of mirror material, weather conditions, geographical location and operational methods. Some general conclusions based on natural and artificial soiling of solar mirrors are:

1) Specular reflectance of a freshly exposed mirror undergoes an initial rapid drop (0.0085 reflectance units/day from 2 day cycle exposure) followed by a decreasing loss rate as the accumulated dust level increases.
2) The long term reflectance loss of uncleaned silvered glass mirrors in Albuquerque is approximately 0.10-0.15 reflectance units with large fluctuations about the average. Similar data at other locations and for other materials are needed.
3) Increased cleaning frequency raises the average reflectance of the mirror.
4) Inverted or vertical storage of the mirrors can significantly reduce the rate of dust accumulation.
5) The effect of weather on the specular reflectance of a mirror depends on the mirror's level of dust accumulation.
6) Dust accumulated upon exposure in the Albuquerque area results in wide-angle scattering of the incident light. The effect on the specular reflectance is primarily to reduce the intensity of the reflected beam while essentially maintaining the shape of its intensity profile.

7) Dust accumulated in the Albuquerque area results in little absorption. The specular reflectance loss to hemispherical reflectance loss ratio is approximately 5 to 1.

8) Scattering caused by accumulated particles increases with decreasing wavelength and increasing level of soiling, with the scattering amplitude increasing below 400 nm, and with the wavelength dependence of dust particle scattering independent of particulate concentration.

9) Small particles ($0.3\ \mu m \lesssim r_p \lesssim 1\ \mu m$) are the most significant source of scattering for the solar spectrum.

10) The concentration of small particles ($r_p \lesssim 5\ \mu m$) tends to increase more rapidly than the concentration of larger particles for mirrors exposed to natural weathering.

11) Decreasing wind velocity increases the relative rate of accumulation of small particles ($r_p \lesssim 5\ \mu m$).

12) Surface coatings and electrostatic biasing can possibly reduce the rate of dust accumulation.

The development of any technique to reduce the rate of soiling of exposed solar mirrors must necessarily involve the optimization of both the operation and design of the mirrors. Long term field test studies will help determine the eventual technique or combination of techniques used.

References

1. Friedlander, S. K., Smoke, Dust and Haze: Fundamentals of Aerosol Behavior (John Wiley and Sons, New York, 1977).
2. Van de Hulst, H. C., Light Scattering by Small Particles (John Wiley and Sons, New York, 1957).
3. Freese, J. M., Effects of Outdoor Exposure on the Solar Reflectance Properties of Silvered Glass Mirrors, Sandia report SAND 78-1649, Sept. 1978.†
4. Arvizu, D. E., "The Solar Central Receiver Test Facility Heliostat Development," presented at Solar Energy Research Institute International Symposium on Concentrator Solar Collection Technology (June 14, 1978), Denver, CO.
5. Pettit, R. B., Solar Energy 19, 733 (1977).
6. Freese, J. M., "Effects of Outdoor Exposure on the Solar Reflectance Properties of Silvered Glass Mirrors," presented at the 1979 International Solar Energy Society Congress (May 28 - June 1, 1979), Atlanta, GA.
7. Forman, S. E., "Endurance and Soil Accumulation Testing of Photovoltaic Modules at Various MIT/LL Test Sites," Report #COO-4094-23 (September, 1978).†
8. Dave King, Sandia Labs., personal communication.
9. Pettit, R. B., Freese, J. M. and Arvizu, D. E., "Specular Reflectance Loss of Solar Mirrors Due to Dust Accumulation," Proceedings of the Institute of Environmental Sciences Solar Seminar on Testing Solar Energy Materials and Systems (May 22-24, 1978), at the National Bureau of Standards, Gaithersburg, MD, pp. 164-168.
10. Edwards, D. K., et al., J. Opt. Soc. Am. 51, 1279 (1961), and Beckman Instructions 1220-B (1962).

11. Taketani, H. and Arden, W. M., "Mirrors for Solar Energy Applications," Proceedings of the 1977 Annual Meeting American Section of ISES (June 6-19, 1977), Orlando, FL, Vol. 1, pp. 5-15 to 5-19, and Vitko, J., Optical Studies of Second Surface Mirrors Proposed for use in Solar Heliostats, Sandia report SAND 78-8228 OUO, April 1978.

12. Huebner, R. H., Arakana, E. T., MacRae, R. A. and Hamm, R. N., J. Opt. Soc. Am. 54, 1434 (1964).

13. Meinel, A. B. and Meinel, M. P., Applied Solar Energy: An Introduction (Addison-Wesley Publishing Co., Menlo Park, CA, 1977).

14. Berg, R. S., Heliostat Dust Buildup and Cleaning Studies, Sandia report SAND 78-0510, March 1978.†

15. Zimon, A. D., Adhesion of Dust and Powder (Plenum Press, New York, 1969).

16. Quantimet 720, Image Analyzing Computers Ltd., Subsidary of Metals Research Ltd., 40 Robert Pitt Drive, Monsey, NY 10952.

17. Gillette, D. A. and Blifford, Jr., I. H., J. Geophys. Res. 79, 4068 (1974).

18. Quenzel, H., J. Geophys. Res. 75, 2915 (1970).

19. Blifford, Jr., I. H. and Ringer, L. D., J. Atmos. Sci. 26, 716 (1969).

20. Standardized Test Dust obtained from A. C. Spark Plug Div., GMC, P. O. Box 1001, Flint, MI 48501.

21. Lapp, M., Penny, C. M. and Asher, J. A., Application of Light-Scattering Techniques for Measurements of Density, Temperature, and Velocity in Gasdynamics, Aerospace Research Laboratories Report ARL 73-0045 (April, 1973).

22. Schumaker and Associates, Inc., "Preliminary Design Report on New Ideas for Heliostat Reflector Cleaning Systems," Sandia Report SAND 79-8181, Aug. 1979.

23. Electrostatic repulsion of dust using a corona discharge system has been investigated by Prof. Stuart A. Hoenig, Dept. of Electrical Engineering, Univ. of Arizona., Tucson, Ariz., 85721.

24. McDonnell Douglas Astronautics Co., Final Report: Cleaning Agents and Techniques for Concentrating Solar Collectors, Sandia report SAND 79-1979, Sept. 1979.[†]

[†]Available from: National Technical Information Service (NTIS), U. S. Department of Commerce, 5285 Port Royal Road, Springfield, VA 22161.

Table 1.

MECHANISMS OF DUST ADHESION

Mechanism	Affecting Material Property
Gravity	Mass
Electrostatic	Surface (coating) conductivity
Charge double layer	Contact potential (difference in work functions)
VanderWalls force	Particle size; Surface roughness
Surface Energy	Solid surface relaxation
Capillary force	Fluid surface relaxation
Chemical/physical bond	Chemical activity

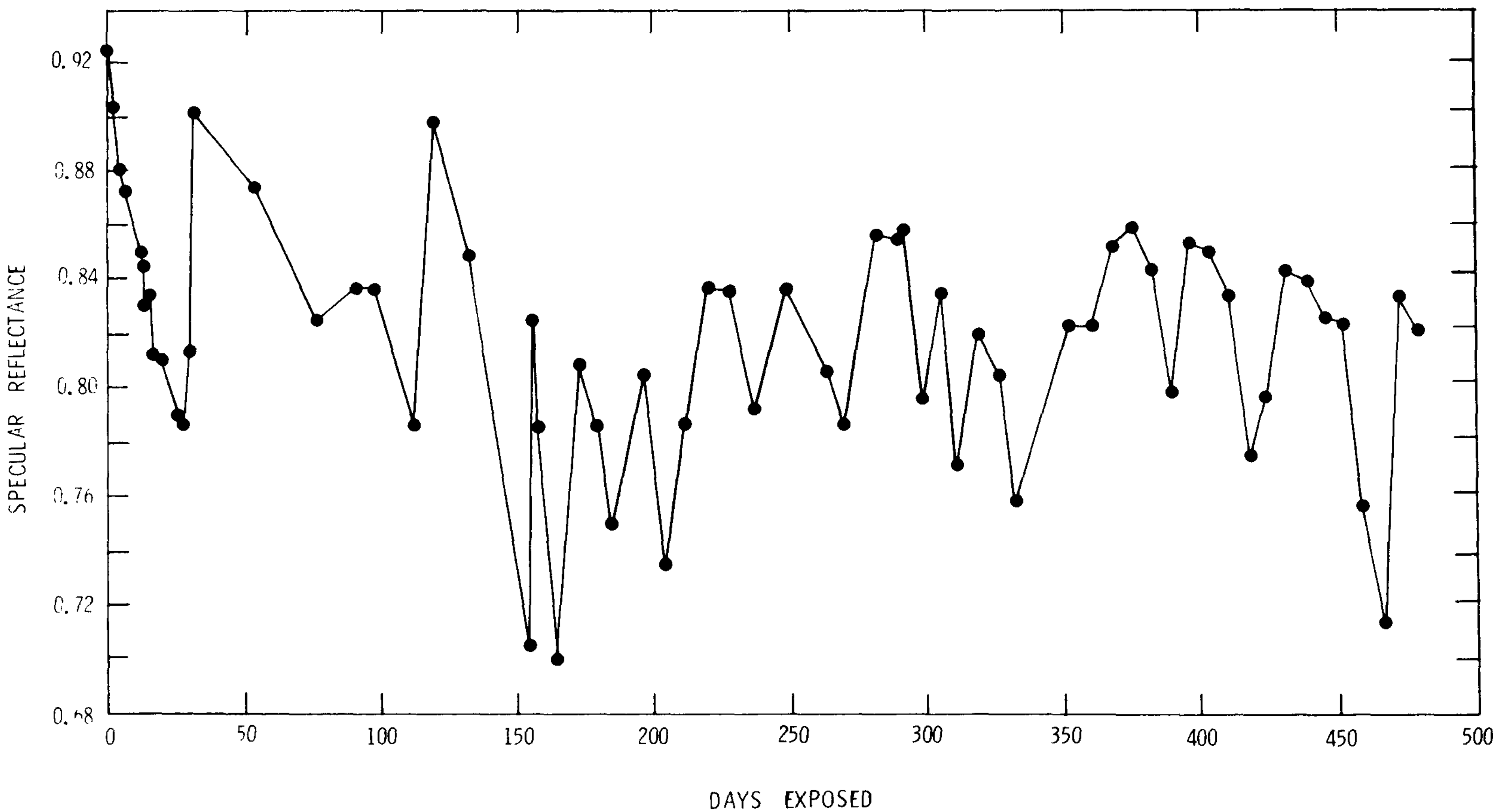
0.92
0.88
0.84
0.80
0.76
0.72
0.68
SPECULAR REFLECTANCE
0
50
100
150
200
250
300
350
400
450
500
DAYS EXPOSED

Figure 1

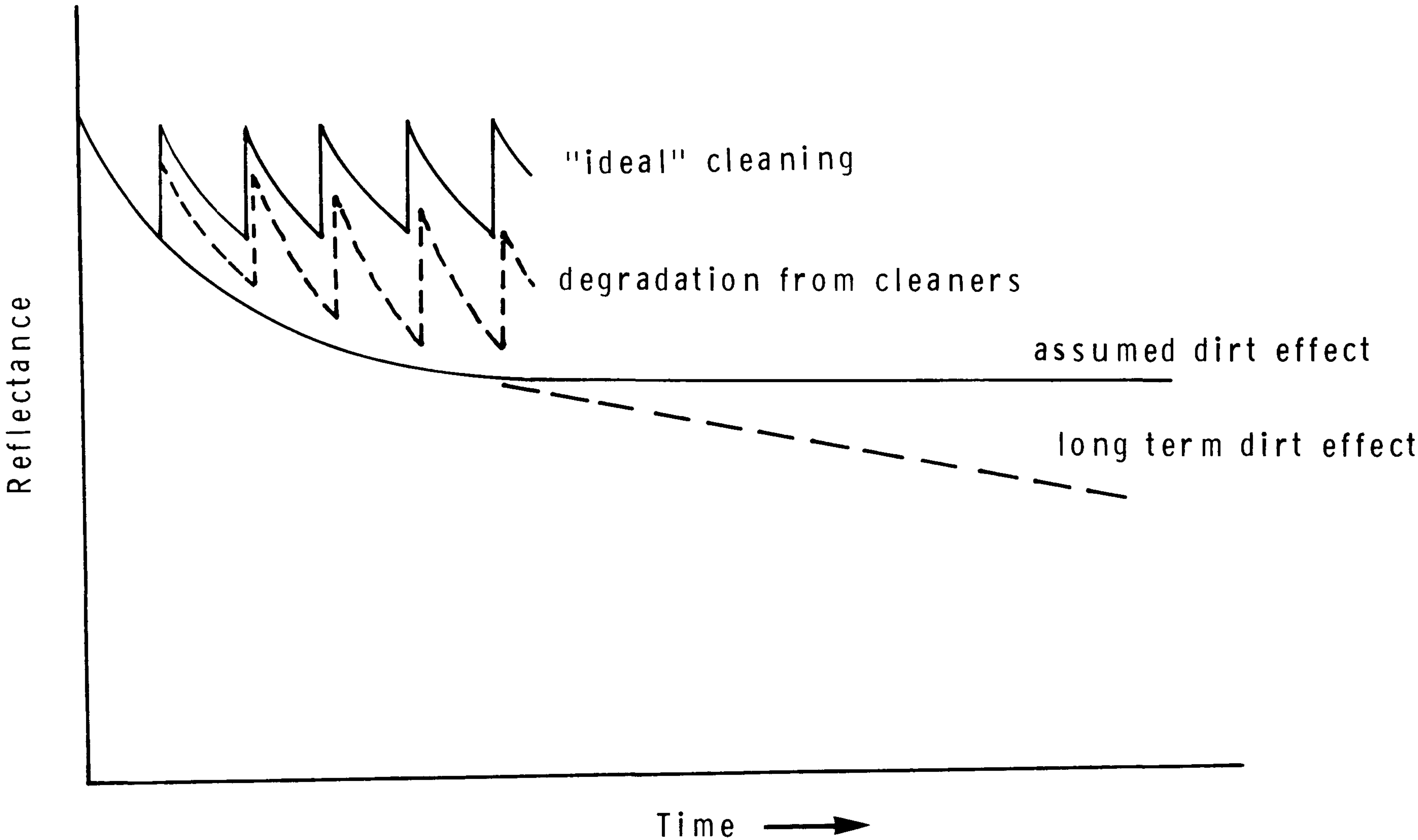
"ideal" cleaning
degradation from cleaners
assumed dirt effect
long term dirt effect
Reflectance
Time

Figure 2

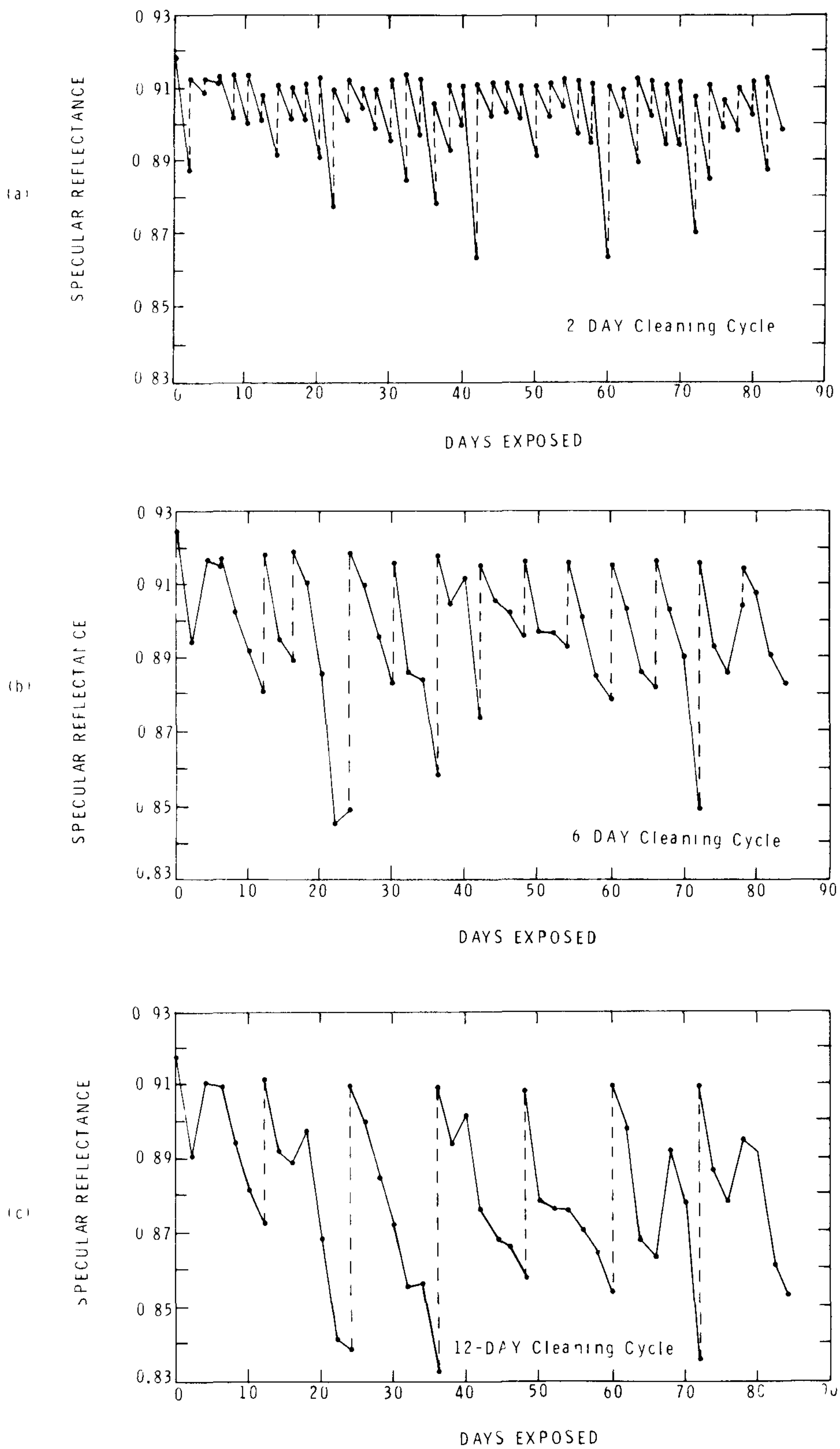

(a)
SPECULAR REFLECTANCE
0.93
0.91
0.89
0.87
0.85
0.83
2 DAY Cleaning Cycle
0
10
20
30
40
50
60
70
80
90
DAYS EXPOSED
(b)
SPECULAR REFLECTANCE
0.93
0.91
0.89
0.87
0.85
0.83
6 DAY Cleaning Cycle
0
10
20
30
40
50
60
70
80
90
DAYS EXPOSED
(c)
SPECULAR REFLECTANCE
0.93
0.91
0.89
0.87
0.85
0.83
12-DAY Cleaning Cycle
0
10
20
30
40
50
60
70
80
DAYS EXPOSED

Figure 3

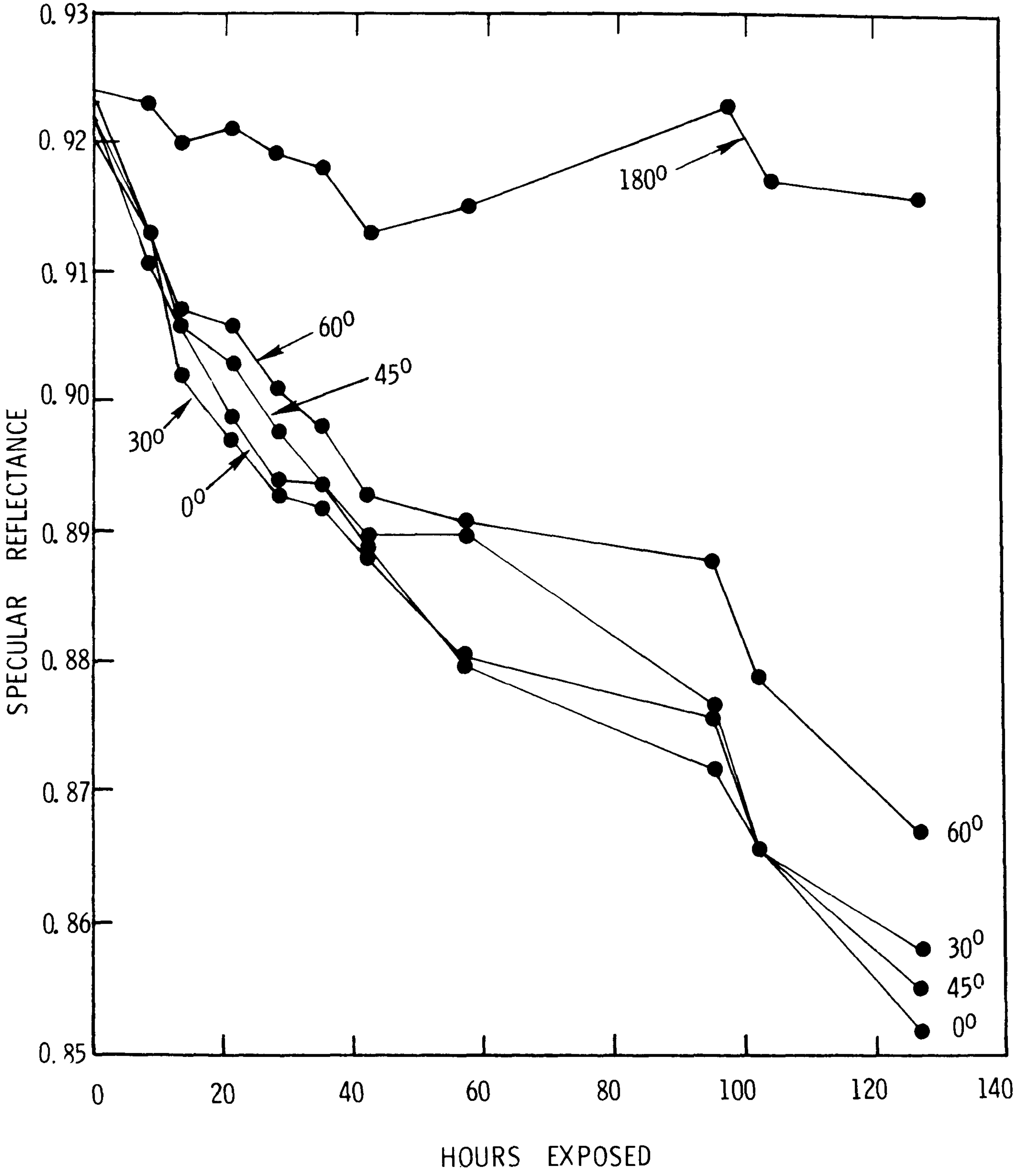
0.93
0.92
0.91
0.90
0.89
0.88
0.87
0.86
0.85
SPECULAR REFLECTANCE
0
20
40
60
80
100
120
140
HOURS EXPOSED
180°
60°
45°
30°
0°
60°
30°
45°
0°

Figure 4

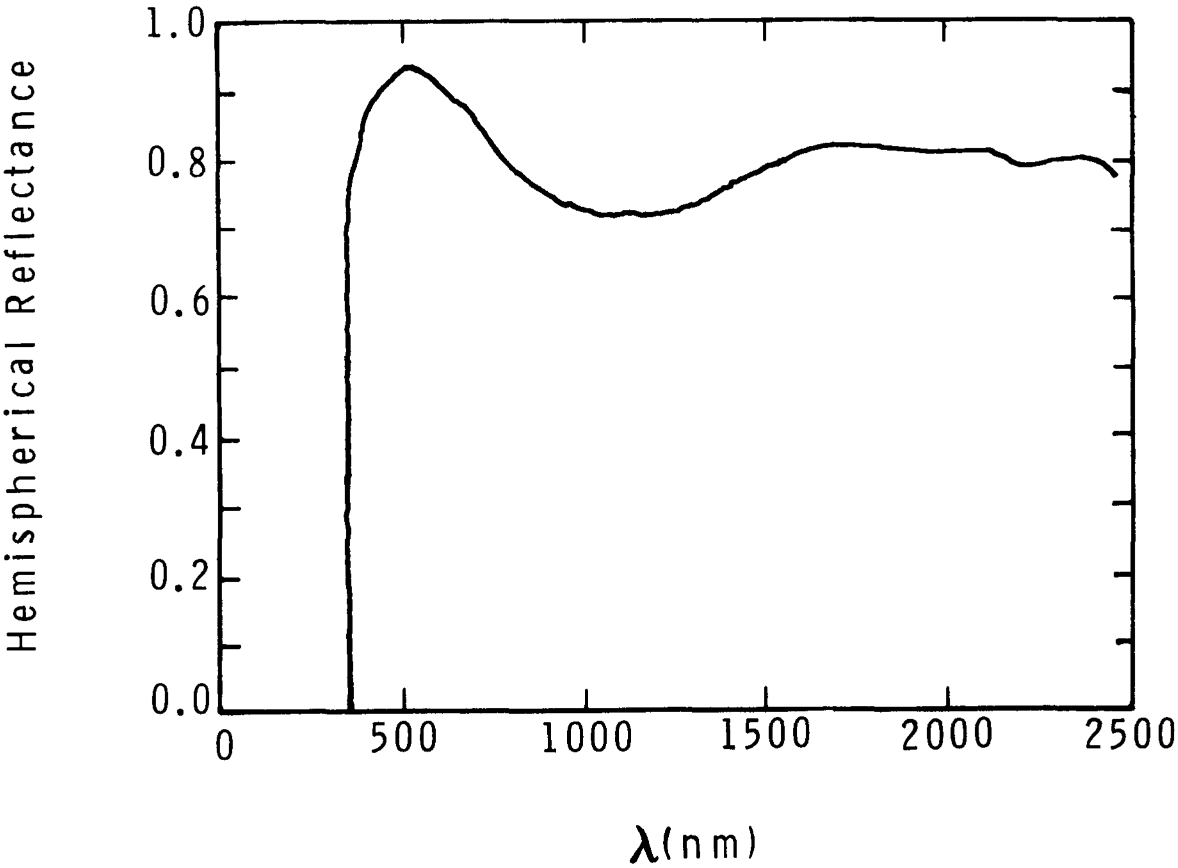

1.0
0.8
0.6
0.4
0.2
0.0
Hemispherical Reflectance
0
500
1000
1500
2000
2500
λ(nm)

Figure 5

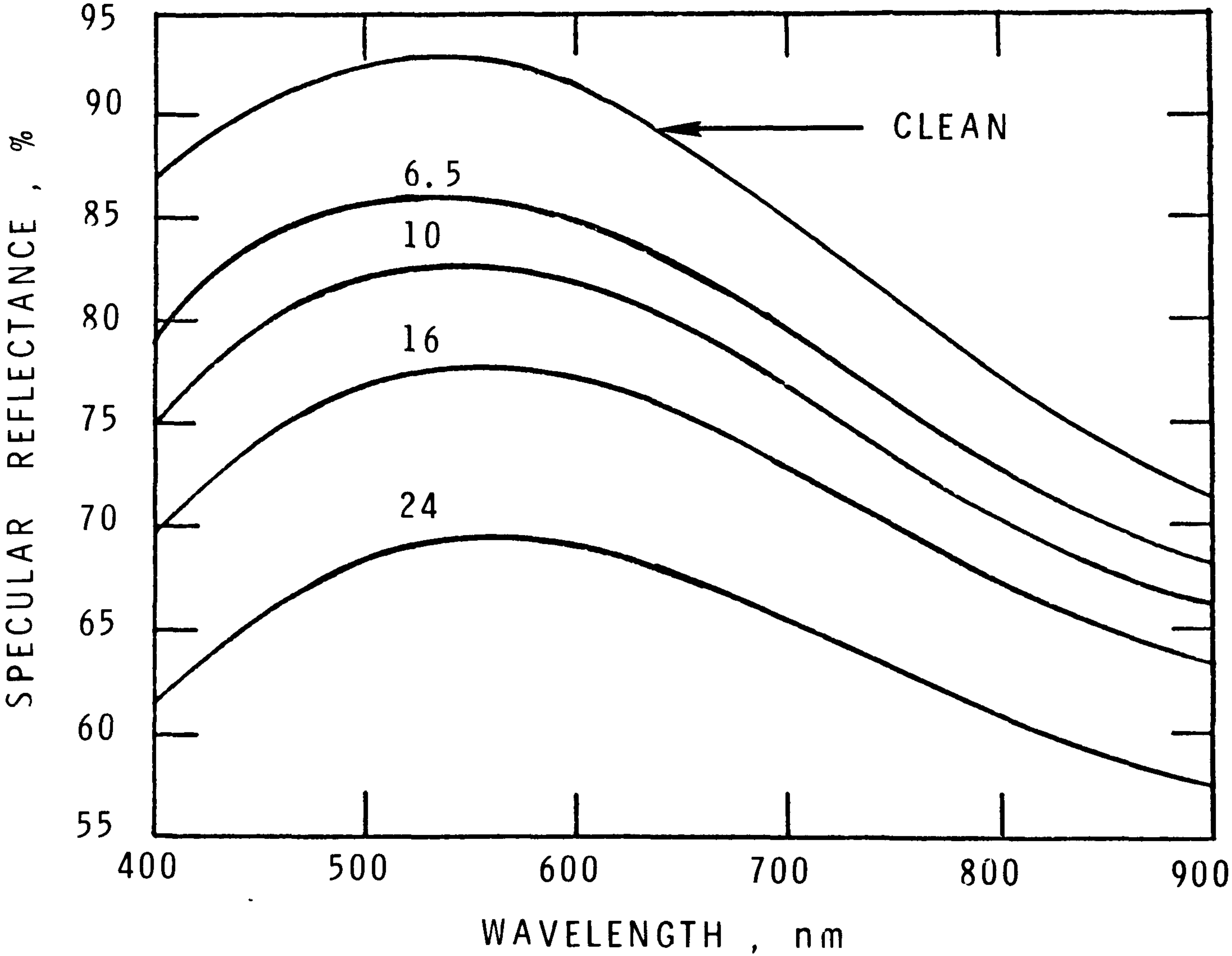
95
90
85
80
75
70
65
60
55
SPECULAR REFLECTANCE , %
CLEAN
6.5
10
16
24
400
500
600
700
800
900
WAVELENGTH , nm

Figure 6

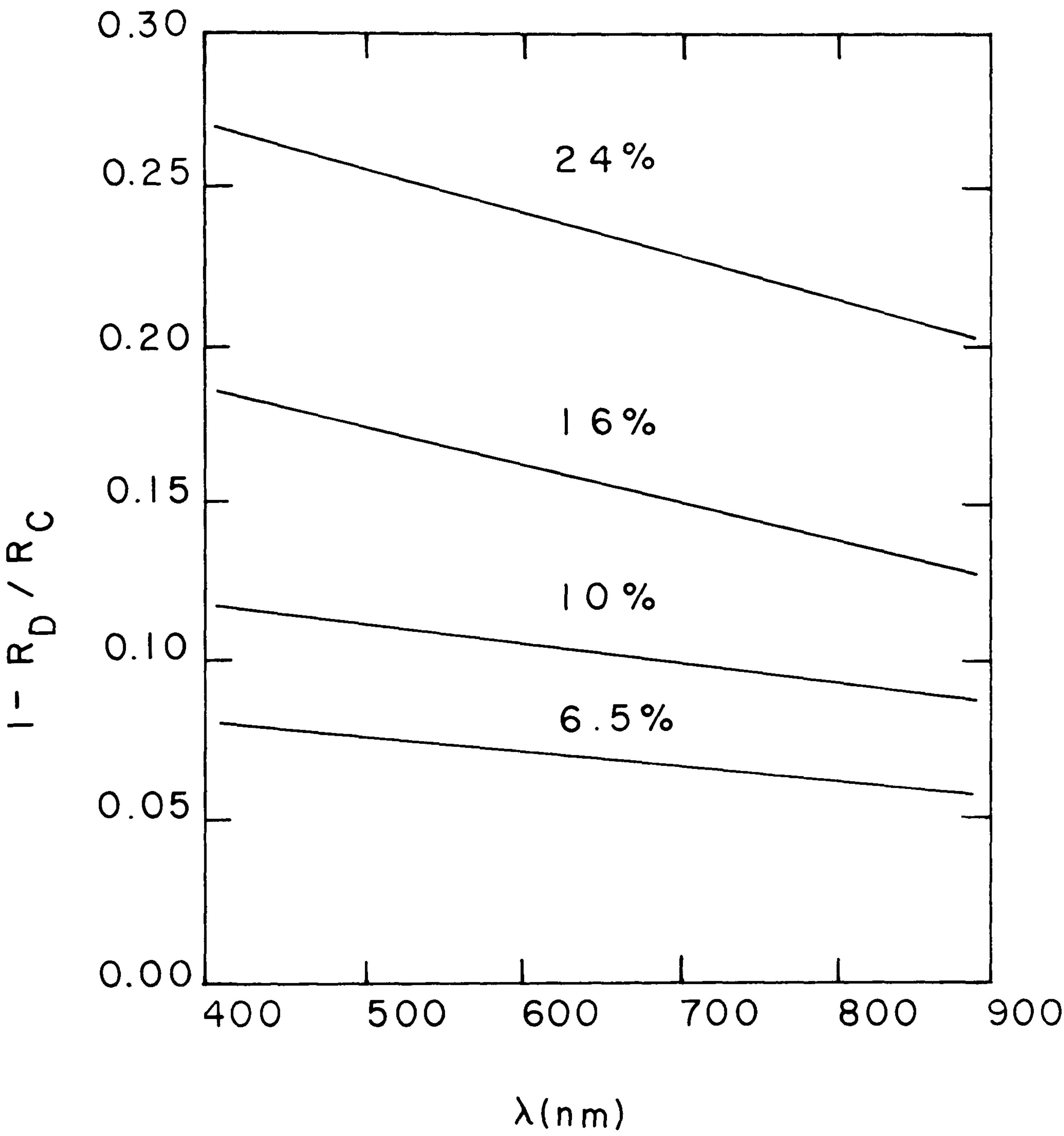
0.30
0.25
0.20
0.15
0.10
0.05
0.00
24%
16%
10%
6.5%
1- R_D / R_C
400
500
600
700
800
900
λ(nm)

Figure 7

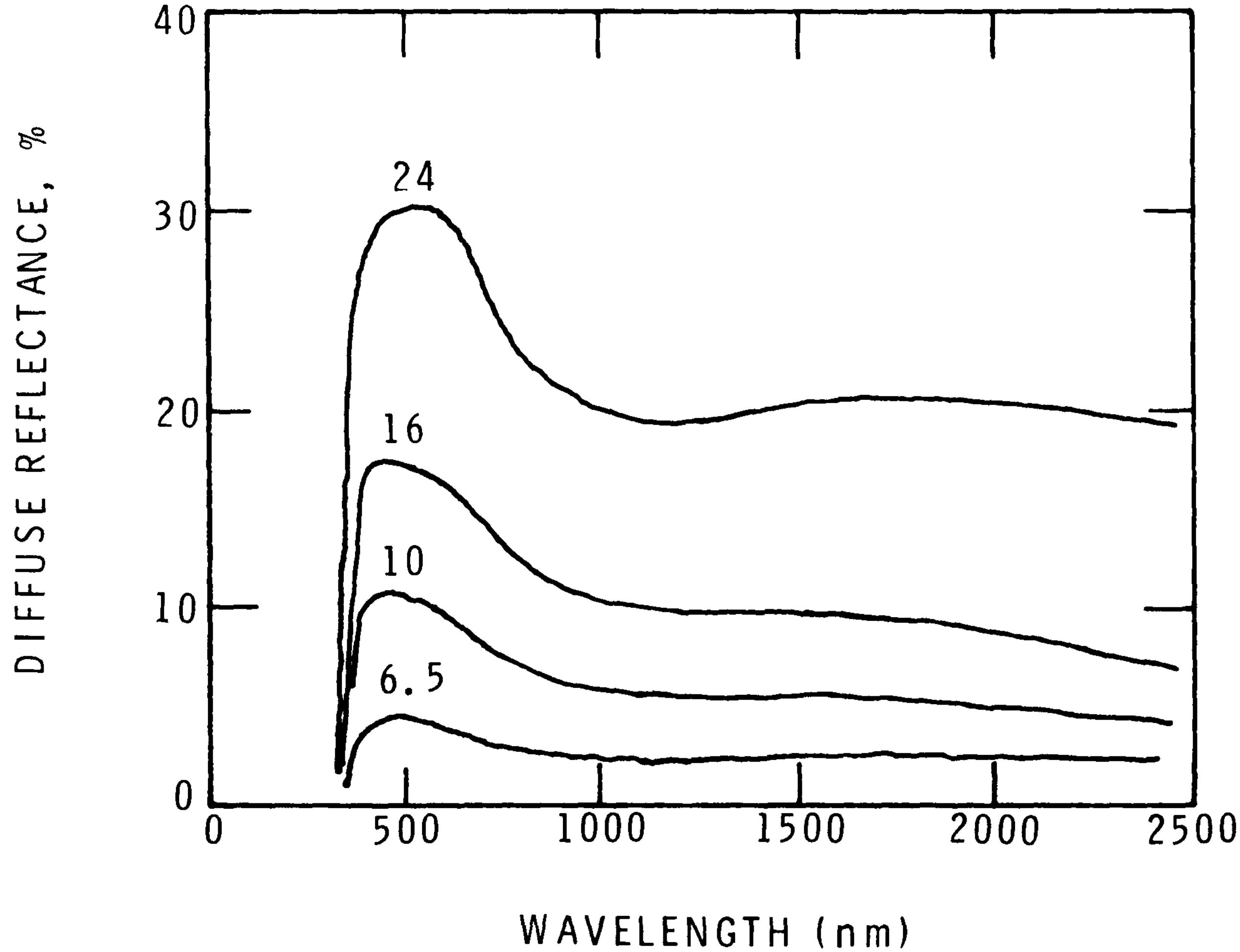
DIFFUSE REFLECTANCE, %
0
10
20
30
40
24
16
10
6.5
0
500
1000
1500
2000
2500
WAVELENGTH (nm)

Figure 8

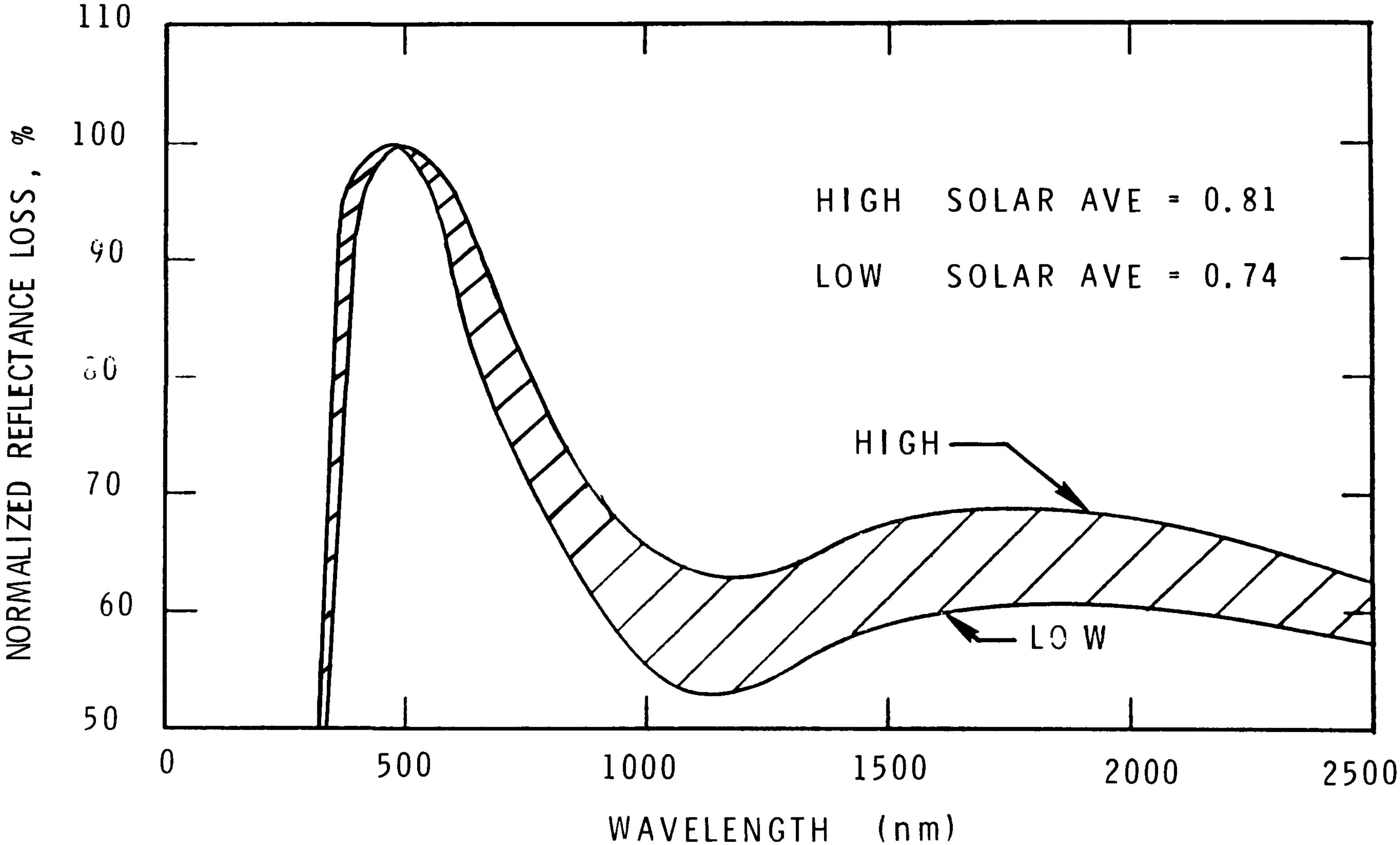

110
100
90
80
70
60
50
NORMALIZED REFLECTANCE LOSS, %
HIGH SOLAR AVE = 0.81
LOW SOLAR AVE = 0.74
HIGH
LOW
0
500
1000
1500
2000
2500
WAVELENGTH (nm)

Figure 9

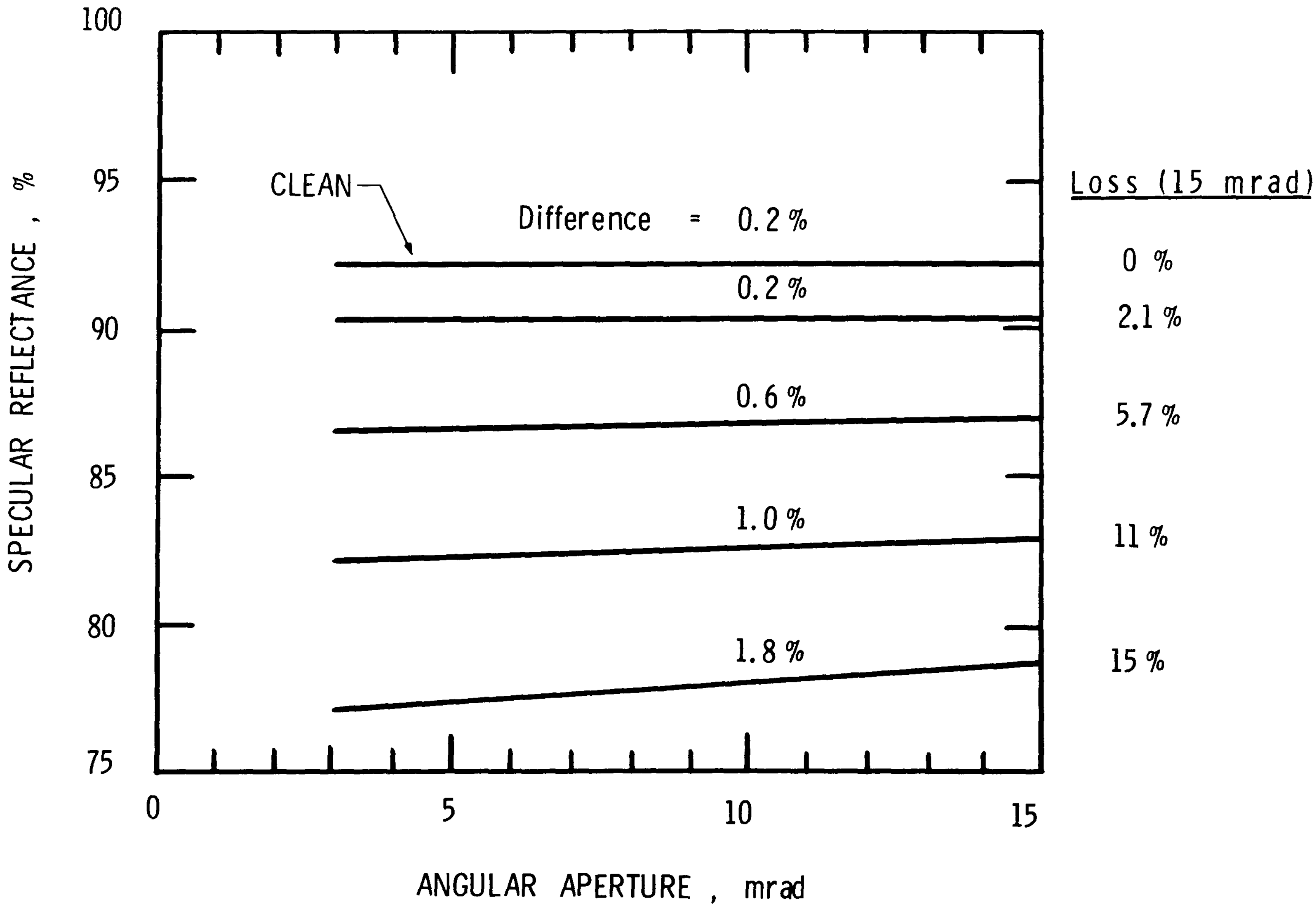
100
95
90
85
80
75
0
5
10
15
SPECULAR REFLECTANCE , %
ANGULAR APERTURE , mrad
CLEAN
Difference = 0.2 %
0.2 %
0.6 %
1.0 %
1.8 %
Loss (15 mrad)
0 %
2.1 %
5.7 %
11 %
15 %

Figure 10

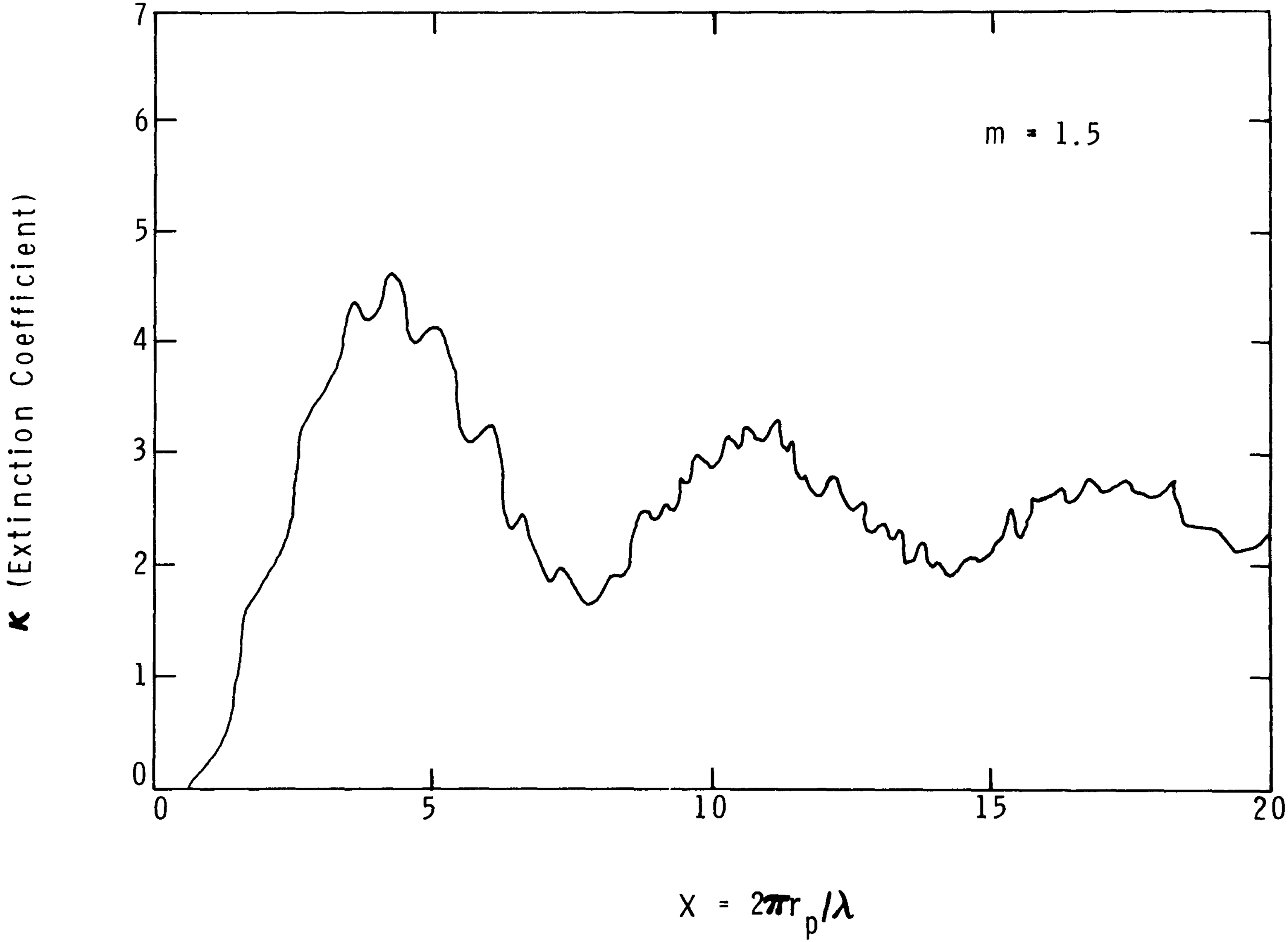

Figure 11

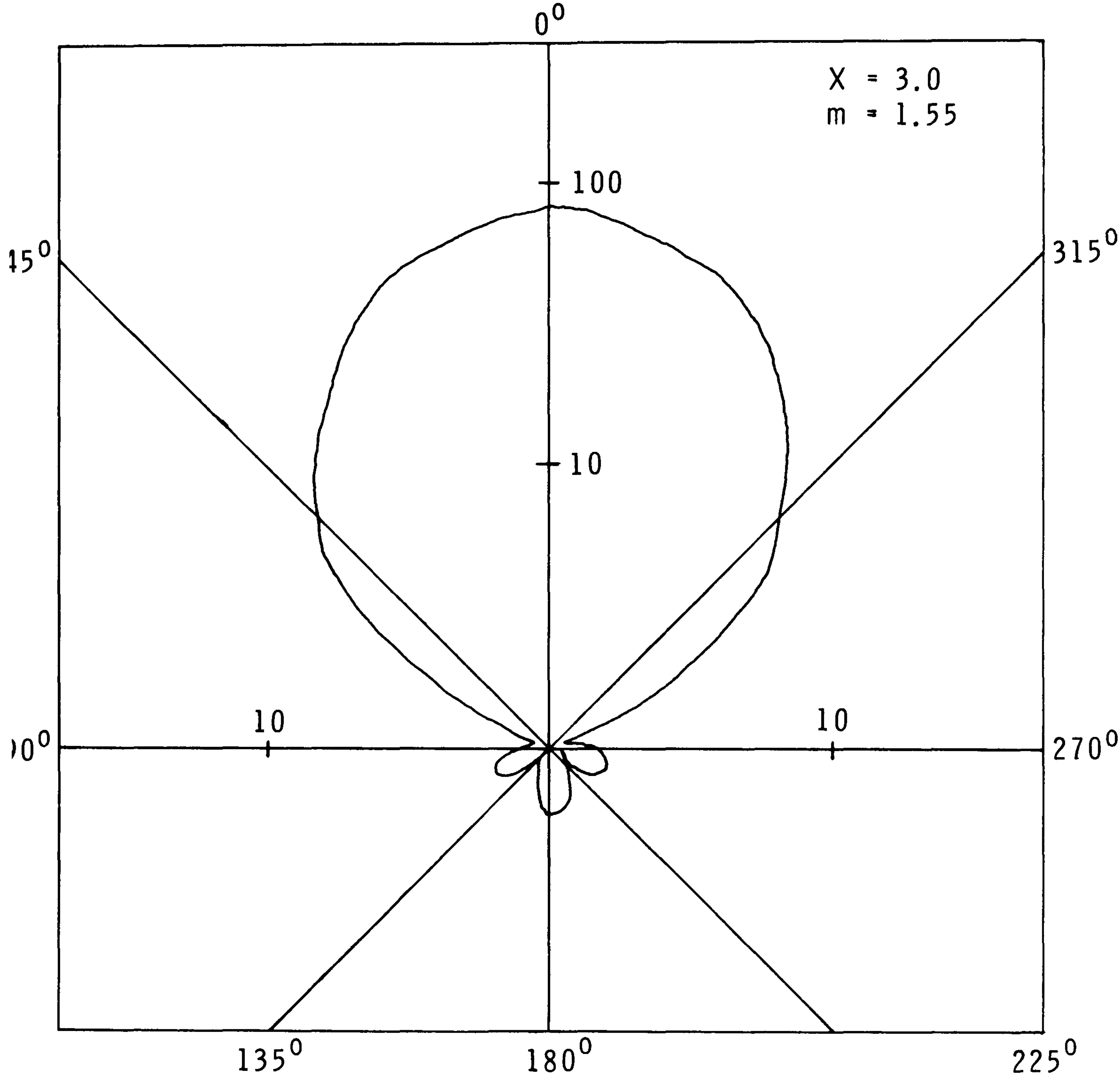

Figure 12

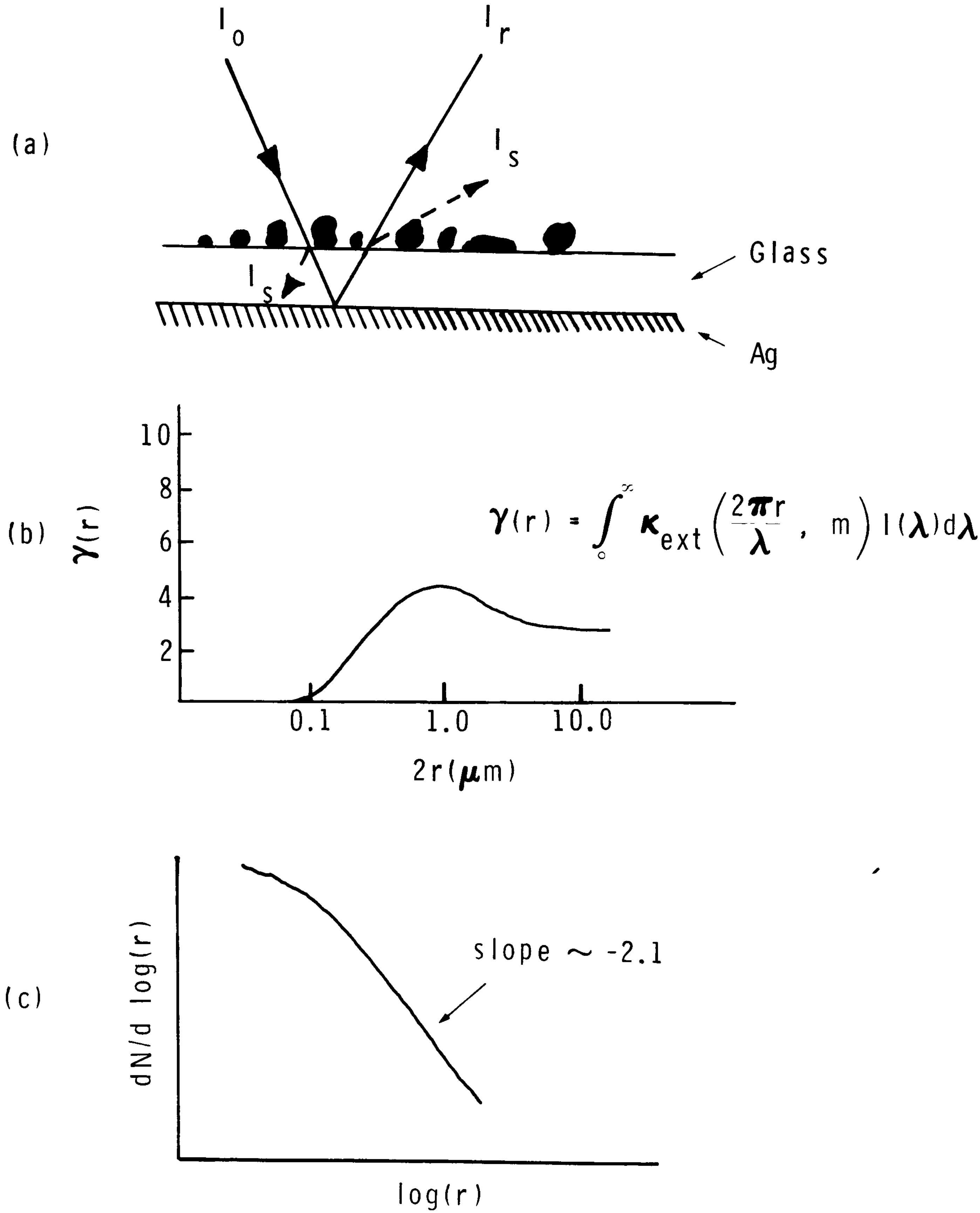
(a)
I
o
I
r
I
s
I
s
Glass
Ag
(b)
γ(r)
10
8
6
4
2
γ(r) = ∫ κ ext (2πr/λ , m) I(λ)dλ
0.1
1.0
10.0
2r(μm)
(c)
dN/d log(r)
slope ~ -2.1
log(r)

Figure 13

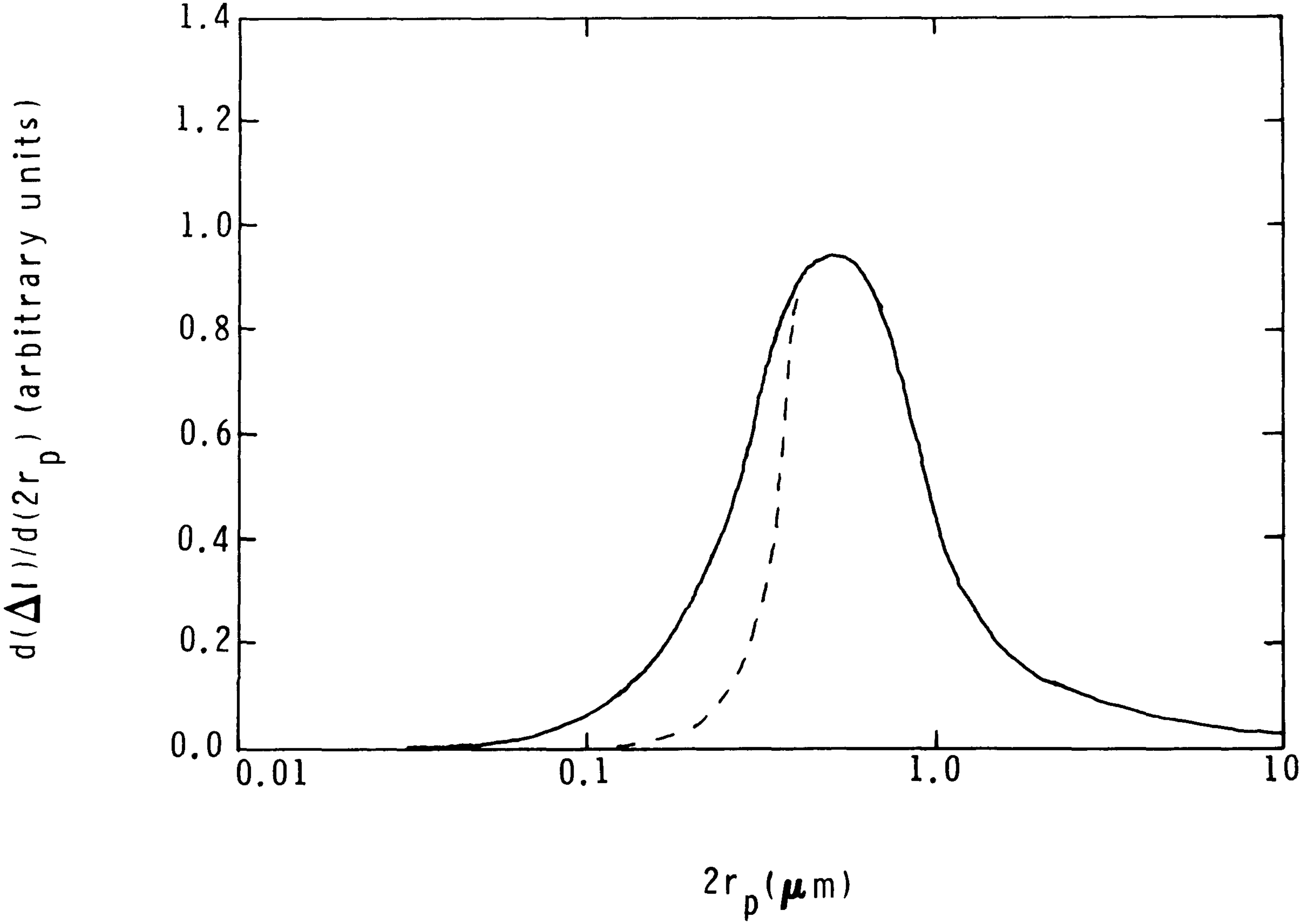
d(ΔI)/d(2r_p) (arbitrary units)
1.4
1.2
1.0
0.8
0.6
0.4
0.2
0.0
0.01
0.1
1.0
10
2r_p(μm)

Figure 14

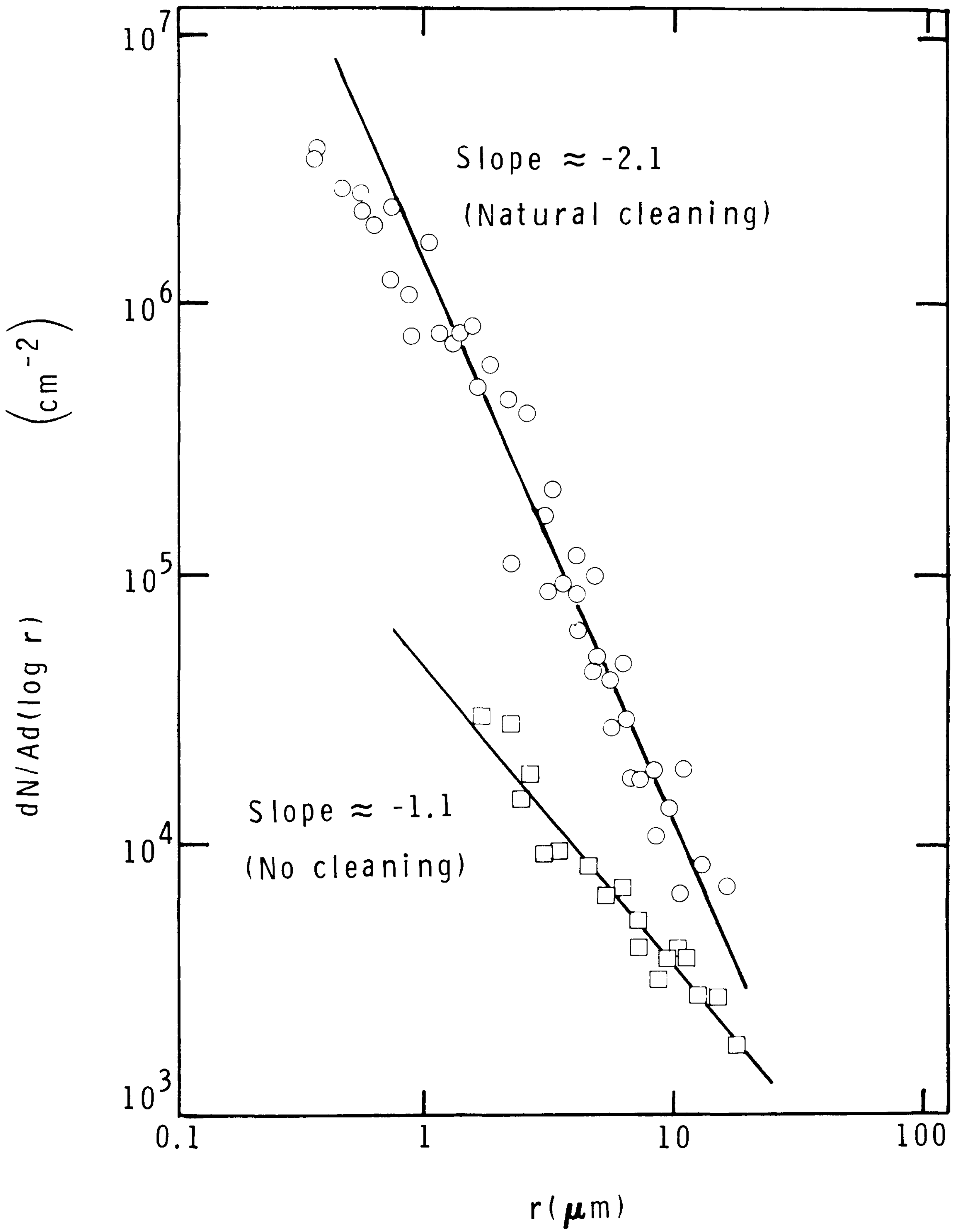

10^7
10^6
10^5
10^4
10^3
dN/Ad(log r) (cm^{-2})
Slope ≈ -2.1
(Natural cleaning)
Slope ≈ -1.1
(No cleaning)
0.1
1
10
100
r(μm)

Figure 15

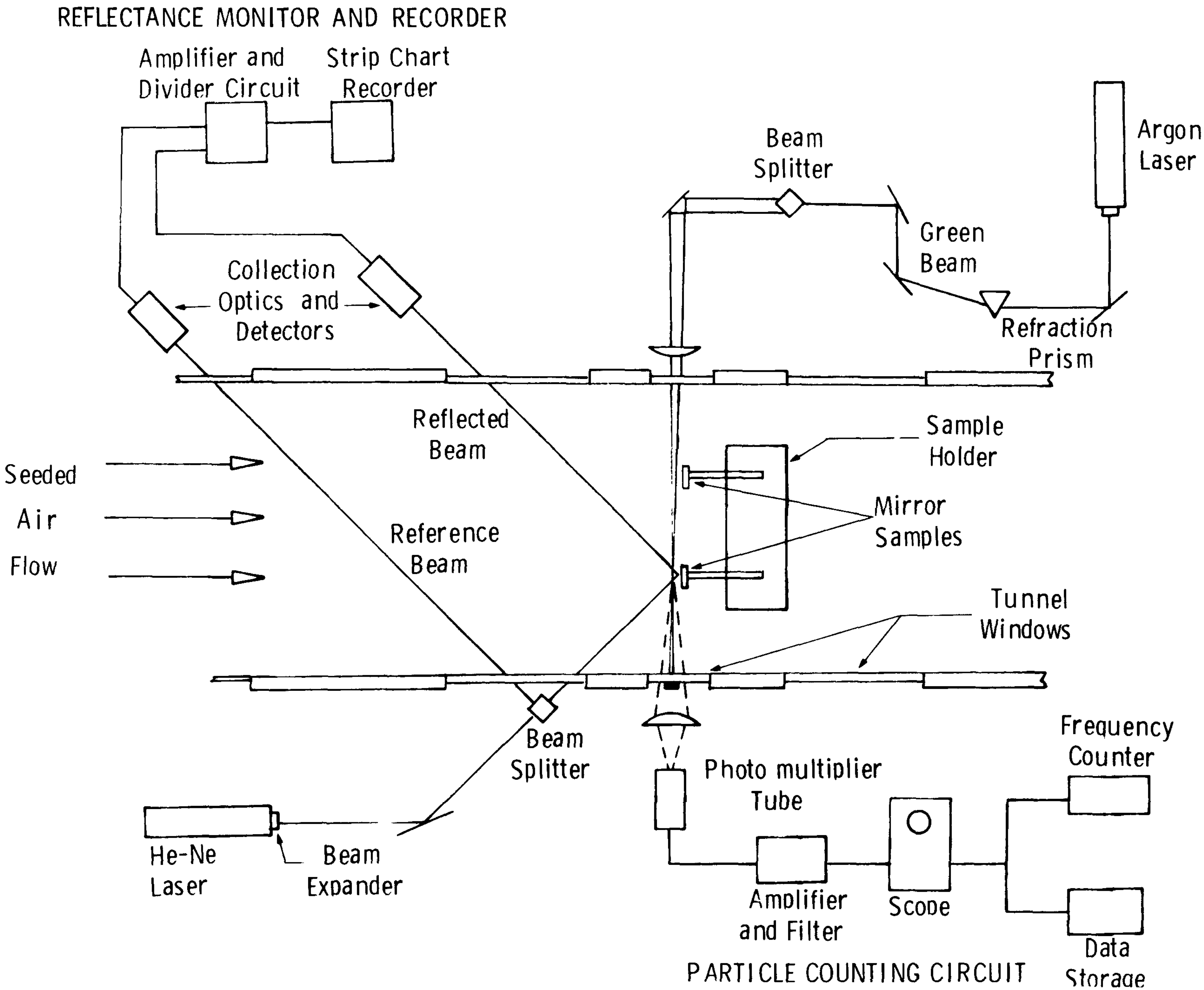
REFLECTANCE MONITOR AND RECORDER
Amplifier and Divider Circuit
Strip Chart Recorder
Beam Splitter
Argon Laser
Green Beam
Refraction Prism
Collection Optics and Detectors
Reflected Beam
Sample Holder
Mirror Samples
Seeded Air Flow
Reference Beam
Tunnel Windows
Beam Splitter
Photo multiplier Tube
Frequency Counter
He-Ne Laser
Beam Expander
Amplifier and Filter
Scope
Data Storage
PARTICLE COUNTING CIRCUIT

Figure 16

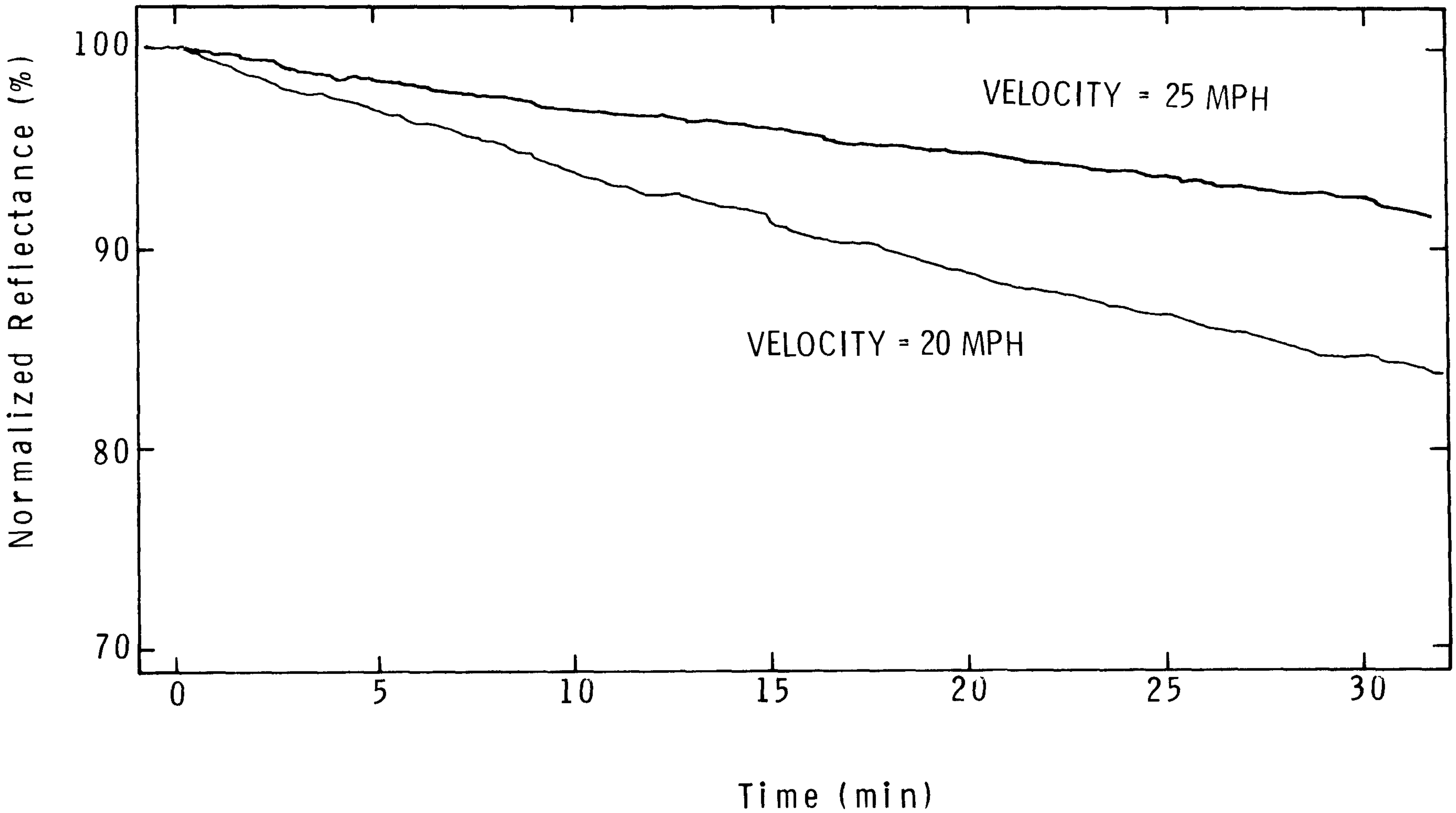
Normalized Reflectance (%)
100
90
80
70
VELOCITY = 25 MPH
VELOCITY = 20 MPH
0
5
10
15
20
25
30
Time (min)

Figure 17

Distribution:

UC-62 (268)

J. Vindum
Acurex Corporation
485 Clyde Avenue
Mountain View, CA 94042

G. Hutchison
Solar Kinetics, Inc.
8120 Chancellor Row
Dallas, TX 75247

V. Reese
Suntec Systems, Inc.
2101 Wooddale Drive
St. Paul, MN 55119

M. Delgado
Del Manufacturing Co.
905 Monterey Pass Road
Monterey Park, CA 91754

J. R. Schuster
General Atomic Company
P. O. Box 81608
San Diego, CA 92138

G. Branch
Hexcel Corporation
11711 Dublin Blvd.
Dublin, CA 94566

A. Stocker
Harrison Radiator Division
General Motors
Lockport, NY

J. F. Britt
Technical Center
General Motors Corporation
Warren, MI 48090

J. Hamilton
Exxon Enterprises
P. O. Box 592
Florham Park, NJ 07923

W. W. Lickhart
Budd Company
Fort Washington, PA 19034

Distribution (contd):

A. F. Shoemaker
Corning Glass Co.
Corning, NY 14830

J. R. Williams
Energy Resources Center
Honeywell, Inc.
2600 Ridgeway Parkway
Minneapolis, MN 55413

M. Faeth
Highland Plating
1128 N. Highland
Los Angeles, CA 90038

H. J. Sund
Ford Aerospace and Communications
3939 Fabian Way
Palo Alto, CA 94303

P. Bender
Ford Glass Division
300 Renaissance Center
P. O. Box 43343
Detroit, MI 48243

W. J. Nagle
Ford Motor Co.
Room E-3184
Scientific Research Labs
Dearborn, MI 48121

R. C. Frounfelter
PPG Industries, Inc.
1 Gateway Center
Pittsburgh, PA 15222

D. L. Thomas
PPG Industries, Inc.
Glass Research Center
Box 11472
Pittsburgh, PA 15238

R. E. Cook
Donnelly Mirrors, Inc.
49 West Third Street
Holland, MI 49423

C. M. Lemrow
Electrical Products Division
Corning Glass Works
Corning, NY 14830

Distribution (contd):

C. G. Lawson
Union Carbide Corp.
P. O. Box X
Oak Ridge, TN 37830

M. Mitchel
Jacobs Engineering Co.
251 South Lake Avenue
Pasadena, CA 91101

J. N. Epel
The Budd Company
Plastic R & D Center
356 Executive Drive
Troy, MI 48084

D. Lombardo
Haveg Industries, Inc.
12827 E. Imperial Highway
Santa Fe Springs, CA 90670

J. Rogan
McDonnell Douglas Astronautics Co.
5301 Bolsa Avenue
Huntington Beach, CA 92647

Solar Energy Research Institute (5)
1536 Cole Blvd.
Golden, CO 80401
Attn: B. Gupta
B. L. Butler
M. Cotton
P. J. Call
K. D. Masterson

U. S. Department of Energy (3)
Albuquerque Operations Office
P. O. Box 5400
Albuquerque, NM 87185
Attn: J. Weisiger
D. N. Pappas
W. P. Grace

U. S. Department of Energy
San Francisco Operations Office
1333 Broadway
Oakland, CA 94612
Attn: W. D. Nettleton

Distribution (contd):

Thomas E. Anderson
DSET Laboratories
Box 1850, Black Canyon Stage
Phoenix, AZ 85029

Jet Propulsion Lab (3)
4800 Oak Grove Drive
Pasadena, CA 91103
Attn: F. L. Bouquet
W. F. Carroll
C. R. Maag

Burton A. Benson
Decorative Products Division
3M Center, Bldg. 209-2N
St. Paul, MN 55101

Cedric Currin
Dow Corning Corp.
Midland, MI 48640

Roger Gillette
Boeing Eng. & Construction
P. O. Box 3707
Seattle, WA 98124

Richard N. Griffin
General Electric
1 River Road
Schenectady, NY 12345

Jacques L. Hull
Acurex Corp.
485 Clyde Avenue
Mountain View, CA 94042

Bob Hahn
Dept. 131
OCLI
P. O. Box 1599
Santa Rosa, CA 95402

Michael A. Lind
Battelle, Pacific NW Labs
Battelle Boulevard
Richland, WA 99352

McDonnell-Douglas (2)
5301 Bolsa Avenue
Huntington Beach, CA 92647
Attn: V. L. Morris
H. Taketani

Distribution (contd):

Stanley W. Moore
LASL, MS-571
Los Alamos, NM 84545

Lloyd Oldham
Martin Marietta Aerospace
P. O. Box 179
Mail #8120
Denver, CO 80201

J. H. Powers
Alcoa Tech Center
Alcoa Center, PA 15069

U. S. Department of Energy (8)
Division of Central Solar Tech.
Washington, D.C. 20545
Attn: G. W. Braun
H. Coleman
M. U. Gutstein
J. E. Rannels
M. E. Resner

U. S. Department of Energy (2)
Agricultural & Industrial Process Heat
Conservation & Solar Application
Washington, D.C. 20545
Attn: W. W. Auer
J. Dolland

1472 L. G. Rainhart
1552 O. J. Burchett
1556 S. A. Ingham
2323 C. M. Gabriel
2324 R. S. Pinkham
2326 G. M. Heck
3161 J. E. Mitchell
3700 J. C. Strassell
4000 A. Narath
4231 J. H. Renken
4700 J. H. Scott
4710 G. E. Brandvold
4713 D. L. King
4713 B. W. Marshall
4719 D. G. Schueler
4720 V. L. Dugan
4721 J. V. Otts
4722 J. F. Banas (25)
4723 W. P. Schimmel
4725 J. A. Leonard

Distribution (contd):

5523	R. C. Reuter
5810	R. G. Kepler
5811	R. A. Assink
5814	F. P. Gerstle
5820	R. E. Whan
5824	J. N. Sweet
5824	R. B. Pettit (4)
5824	E. P. Roth (4)
5824	J. M. Freese
5830	M. J. Davis
5840	N. J. Magnani
8450	R. C. Wayne
8451	P. J. Eicker
8342	J. Vitko, Jr.
8453	W. G. Wilson
3141	T. L. Werner (5)
3151	W. L. Garner (3) For DOE/TIC (Unlimited Release)
3154-3	R. P. Campbell (25)
6011	G. C. Newlin (3)
8266	E. A. Aas (2)